PRODUCTION AND CHARACTERIZATION OF DIATOMACEOUS EARTH-BASED GEOPOLYMERS AND GEOPOLYMERIC MORTARS

JÚLIA FERREIRA MURTA

Master thesis report submitted to:

ESTIG – Escola Superior de Tecnologia e Gestão

IPB – Instituto Politécnico de Bragança

Master's degree in:

Chemical Engineering

Supervisors:

Prof. Doutor Helder Gomes (IPB)

Prof. Doutora Débora Macanjo (IPB)

Prof. Doutor Carlos Eduardo dos Santos (CEFET-MG)

BRAGANÇA - PORTUGAL

JUNE, 2023

PRODUCTION AND CHARACTERIZATION OF DIATOMACEOUS EARTH-BASED GEOPOLYMERS AND GEOPOLYMERIC MORTARS

JÚLIA FERREIRA MURTA

Thesis report submitted to **Escola Superior de Tecnologia e Gestão** of **Instituto Politécnico de Bragança** to obtain the Master's Degree in **Chemical Engineering** in the ambit of the double diploma with the **Centro Federal de Educação Tecnológica – Minas Gerais**

Supervisors:

Prof. Doutor Helder Gomes (IPB)

Prof. Doutora Débora Macanjo (IPB)

Prof. Doutor Carlos Eduardo dos Santos (CEFET-MG)

BRAGANÇA - PORTUGAL

JUNE, 2023

ACKNOWLEDGEMENTS

Firstly, I would like to express my gratitude to my mother and late father for their whole support throughout my life. No one has believed in my potential as much as you both, and your investment in my education has made all the difference, allowing me to reach where I am today. I would also like to thank my siblings, Leonardo, Nathália, and Vinícius, for the joyful moments they have granted me in life. Additionally, I extend my appreciation to my friends in Brazil, Fernanda, Thalita, Rafael, Carol, Henrique, Aninha, and Ana, as well as my friends from the exchange program, Lara, Paloma, Ana, Marcos, Danilo, Vinicius, Renata, and Vitor, for their incredible support during this time.

Thanks to my supervisors, Professor Dr. Helder Teixeira Gomes and Professor Dr. Débora Macanjo of Instituto Politécnico de Bragança (IPB), I sincerely value the support and trust given to me. Furthermore, I would like to thank my advisor, Dr. Carlos Eduardo dos Santos, from Centro Federal de Educação Tecnológica de Minas Gerais (CEFET-MG). Throughout my academic journey, both during college and my master's degree, his guidance and assistance really helped me with my professional development.

A very special thanks to Me. Ana Paula Ferreira da Silva, who was essential for the successful completion of this project. Without her support, teachings, and advice, I would not have been able to attain my objectives.

I would like to thank CEFET-MG for awarding me the scholarship and providing support throughout my relocation to Portugal. Thanks to IPB for giving me the chance of doing this double degree. This incredible opportunity has had a profound impact on my personal and professional development, allowing me to live one of my biggest dreams.

Last, but no less important, I would like to thank the Foundation for Science and Technology (FCT, Portugal) for financial support through national funds FCT/MCTES (PIDDAC) to CIMO (UIDB/00690/2020 and UIDP/00690/2020) and SusTEC (LA/P/0007/2020). This work is also a result of the project "BacchusTech - Integrated Approach for the Valorisation of Winemaking Residues" (POCI-01-0247-FEDER-069583), supported by the Competitiveness and Internationalization Operational Programme (COMPETE 2020) under the PORTUGAL 2020 Partnership Agreement, through the European Regional Development Fund.

ABSTRACT

Since 1980, the world has faced an increase in the earth's average surface temperature due to the high release of carbon dioxide into the atmosphere. One of the main responsible for this CO_2 release is the manufacture of Portland Cement, associated with a carbon dioxide emission of around 7% of the world's total emissions. In this way, there is a need to find alternatives to Portland cement to reduce these emissions. This work aims to contribute to this endeavor, proposing the application of a solid waste used as a wine filtration agent in the wine industry, diatomaceous earth, containing high amounts of silicon, to produce geopolymers and geopolymeric mortars. A geopolymer is an inorganic polymer produced with an aluminosilicate precursor reacted with an alkaline solution that has been studied as an alternative to cement in the composition of mortars and concretes. Diatomaceous earth and alumina were employed in this work as aluminosilicate sources for the geopolymer precursor, while sodium hydroxide and sodium silicate were used as the alkaline solution. The production process involved mixing all these raw materials of the geopolymers to create a fresh geopolymer, which was then combined with sand and water to form a mortar. In some instances, a specific amount of cement was also added to the binder along with the geopolymer. Subsequently, the samples underwent a 28-day curing process, with the initial four days placed in an oven at 40 ºC and then transferred to room temperature. Following production, the geopolymers were characterized using XRD, FTIR, SEM-EDS, and pore property analysis. On the other hand, the mortar samples underwent compressive and flexural strength tests and a flow test. The results revealed that the most favorable mortar sample, sample 2 (S2), utilized the top-performing geopolymer sample, Geopolymer 2 (GP2), as the geopolymeric binder. GP2 featured a NaOH concentration of 10 M, and a Si/Al ratio of 3,5. In the case of the S2 mortar, it consisted of 75% GP and 25% Portland Cement in the binder. This combination resulted in a higher proportion of geopolymer phase, consequently improving mechanical properties.

Keywords: Geopolymers; Spent diatomaceous earth; Mortar; Solid waste.

RESUMO

Desde 1980, o mundo vem enfrentando um aumento na temperatura média da superfície terrestre devido à alta emissão de dióxido de carbono na atmosfera, tendo como um dos principais responsáveis a indústria de cimento Portland (PC), que tem associada a sua produção uma emissão de CO_2 responsável por cerca de 7% do total do mundo. Assim, é necessário encontrar alternativas ao PC a fim de reduzir essas emissões. Este trabalho tem como objetivo contribuir para esse esforço, propondo a aplicação de um resíduo sólido chamado terra diatomácea, utilizado como meio de filtração do vinho na indústria vinícola e que contém altas quantidades de silício, para produzir geopolímeros e argamassas geopoliméricas. Um geopolímero é um polímero inorgânico produzido com um precursor aluminossilicato reagido com uma solução alcalina que tem sido estudado como uma alternativa ao cimento na composição de argamassas e concretos. Neste trabalho, foram utilizadas a terra diatomácea e a alumina como fontes de aluminossilicato para o precursor do geopolímero, enquanto o hidróxido de sódio e o silicato de sódio foram usados como solução alcalina. O processo de produção envolveu inicialmente a mistura de todas essas matérias-primas para criar um geopolímero fresco, que foi então combinado com areia e água para formar uma argamassa. Em certos casos, uma quantidade específica de cimento também foi adicionada ao ligante juntamente com o geopolímero. Posteriormente, as amostras passaram por um processo de cura de 28 dias, sendo os quatro primeiros dias em um forno a 40 ºC e depois transferidas para a temperatura ambiente. Após a produção, os geopolímeros foram caracterizados por XRD, FTIR, SEM-EDS e análise das propriedades texturais. As amostras de argamassa, por sua vez, foram submetidas a testes de resistência à compressão e flexão, bem como a um teste de fluidez. Os resultados revelaram que a amostra de argamassa mais favorável, a amostra 2 (S2), utilizou o geopolímero de melhor desempenho, o Geopolímero 2 (GP2), como ligante geopolimérico. O GP2 apresentava uma concentração de NaOH de 10 M e uma relação Si/Al de 3,5. No caso da argamassa S2, ela era composta por 75% de GP e 25% de cimento Portland como ligante. Essa combinação resultou em uma proporção maior de fase geopolimérica, consequentemente levando a melhorias nas propriedades mecânicas.

Palavras-chave: Geopolímeros; Terra diatomácea; Argamassa; Resíduo sólido.

LIST OF CONTENTS

LIST OF FIGURES

LIST OF TABLES

LIST OF ABBREVIATIONS

ASTM	American Society for Testing and Materials
BJH	Barrett-Joyner-Halenda
CASH	calcium Aluminate Silicate Hydrate
CIMO	Mountain Research Centre
(C,N)-A-S-H	Calcium Substituted NASH Gels
CE	Circular Economy
C-S-H	Calcium-Silicate-Hydrate
DE	Diatomaceous Earth
FA	Fly Ash
FCC	Fluid Catalytic Cracking
FTIR	Fourier Transform Infrared Spectroscopy
GGBFS	Ground Granulated Blast Furnace Slag
GBFS	Granulated Blast Furnace Slag
GHGs	Greenhouse Gases
GLSS	Granulated Lead Smelter Slag
ICP-OES	Inductively Coupled Plasma - Optical Emission Spectrometry
MK	Metakaolin
NASH	Sodium Alumino-silicate Hydrate
NS	Nano Silicate
OPA	Oil Palm Ash
PC	Portland Cement
PVA	Polyvinyl Acetate

RHA	Rice Husk Ash
RM	Red Mud
S_{BET}	Specific Surface Area
SDE	Spent Diatomaceous Earth
SEM-EDS	Scanning Electron Microscopy with Energy Dispersive X-ray Spectroscopy
SF	Silica Fume
SS	Sodium Silicate
XRD	X-ray diffraction

1. INTRODUCTION

Since the industrial revolution, the world has faced consequences of industrial expansion and fossil fuel combustion, such as the accumulation of greenhouse gases (GHGs) in the atmosphere[1]. The carbon dioxide (CO_2) concentration has significantly increased in the atmosphere by 30% since 1950[2], caused most likely by human activities, such as forestation for agriculture and forestry[2], industrialization[3], and transportation[4]. Figure 1 shows the concentration of CO_2 in the atmosphere throughout history until 2013.

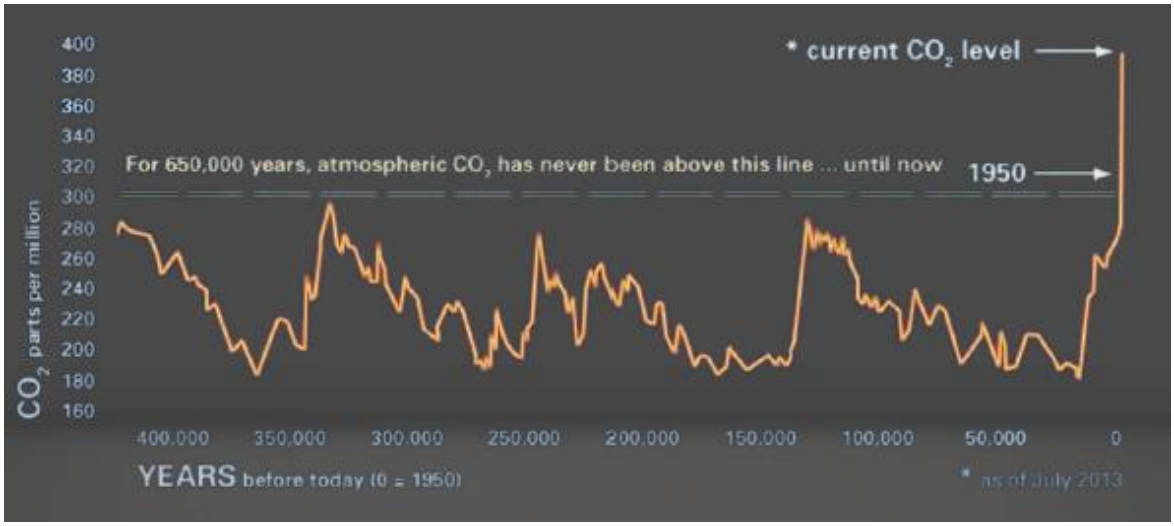

Figure 1: The concentration of carbon dioxide in the atmosphere (adapted)[5].

One of the worst consequences of this event is the change in the earth's temperature. Scientists showed that since 1880, the earth's surface average temperature has increased by about 0,8 ºC, with a tendency to keep rising as humankind continues its environmentally harmful activities, especially burning fossil fuel[5]. This temperature rise is causing intensive damage to the world, how we live, and nature. Plants and animals need specific conditions to survive and grow, including a suitable ambient temperature and enough water. Heat waves and floods are becoming more frequent and intensive, increasing human and material casualties. In addition, snow and ice are melting, causing sea levels to rise and the transformation of sunlight-reflecting surfaces (snow surfaces) to sunlight-absorbing surfaces, so more energy is trapped in the earth's atmosphere[5].

The building sector appears among the most responsible for this situation, accounting for almost 38% of the total CO_2 emissions[5,6]. Portland Cement (PC)-based materials are the second most used substances in the world after water. Buildings, bridges, and roads would be impossible without these materials. Because of this, cement is the

most extensively manufactured product worldwide, with a global annual production of about 4 billion tons. This manufacturing consumes a massive amount of energy and raw materials. Besides, in 2021, the cement industry emitted nearly 2,9 billion tons of carbon dioxide, which is more than 7% of the global carbon emissions[7–12].

Nevertheless, the projected urbanization for the next 50 years indicates that the global urban population will increase by 2,5 billion, mainly in Asia and Africa. Considering the already housing deficit and the lack of infrastructure with this population growth, the demand for Portland Cement and concrete will continue to increase over the years[11], and developing countries such as India will produce even more, as shown in Figure 2[13]. That's why it is necessary to create strategies to limit this environmental impact.

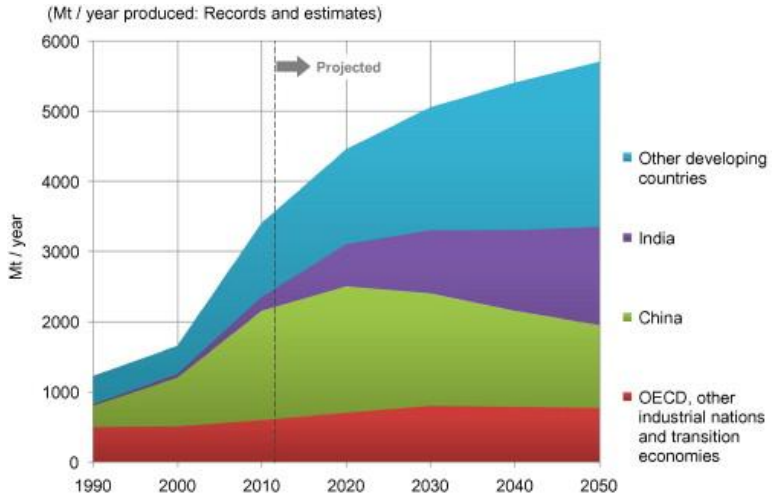

Figure 2: World Portland cement production 1990–2050[13].

Some of the alternatives to PC are (i) the partial replacement of this material, (ii) the production of alternative low-energy cement, e.g., calcium sulfoaluminates, or (iii) the formulation of new binders, such as alkali-activated materials. This latter type is mainly known as geopolymer (GP), which has a wide range of applications as a PC substitute due to its properties, such as enhanced mechanical properties and the ability to withstand elevated temperatures and chemical attacks by acids and acidsalts[14].

Geopolymeric cement is a kind of green cement that possesses significant environmental benefits, cannot only effectively recycle solid waste and save many resources, and has low energy consumption and carbon footprint. Therefore, geopolymer is an alkali-activated binder made by alkali activation of aluminosilicate source materials such as fly ash (FA), metakaolin (MK), diatomaceous earth (DE), among other sources.

The CO_2 emission by geopolymers is said to be 80% lower compared to the production of ordinary Portland cement[8,15].

Among the solid waste, Diatomaceous Earth can be used as an aluminosilicate precursor in geopolymers. This earth is used in the wine industry, and it's commonly thrown away after wine production. So, using this spent DE as a component of a geopolymer that will be used to replace cement on mortars can be a possibility to reduce environmental impacts. This dissertation studies this possibility, presenting these geopolymer's compositions and analysing the mechanical strength of a spent diatomaceous earth-based geopolymeric mortar.

1.1. DOCUMENT STRUCTURE

This state-of-the-art report is divided into four chapters. Chapter 1 introduces the background of the work to be done in the master thesis project, presenting relevant topics for understanding the theme regarding the impact of cement production, the alternatives for this material, and the use of geopolymers to replace cement. Then, the general and specific objectives of this work are detailed.

Chapter 2 presents explicitly the state-of-the-art, where important literature about conventional building materials, their environmental impact, mortars, geopolymers, diatomaceous earth, and geopolymeric mortars are studied.

In Chapter 3, the objectives are pointed out, presenting the general and the specific objectives.

In Chapter 4, the methodology of this work is detailed, where reagents and equipment are presented, and the methods of producing geopolymers and mortars are described, as well as the method of characterization of these materials.

The results obtained for the characterization of the produced geopolymers and geopolymeric mortars are presented in Chapter 5.

Finally, chapter 6 presents the conclusions with topics of interest for future research.

2. STATE OF THE ART

2.1. PORTLAND CEMENT AND MORTAR

Portland cement is a mixture of compounds produced by burning limestone and clay in a rotary oven at around 1450 ºC. In more detail, during this production (illustrated in Figure 3), there is a step called calcination, described by equation 1, which is the decomposition of calcium carbonate (limestone) to calcium oxide (lime) to produce basic cement[13]. The obtained product is called clinker in the cement business, a powder that reacts with water and changes from a paste or liquid solution into a solid mass.

$$3CaCO_3 + SiO_2 \rightarrow Ca_3SiO_5 + 3CO_2 \qquad (1)$$

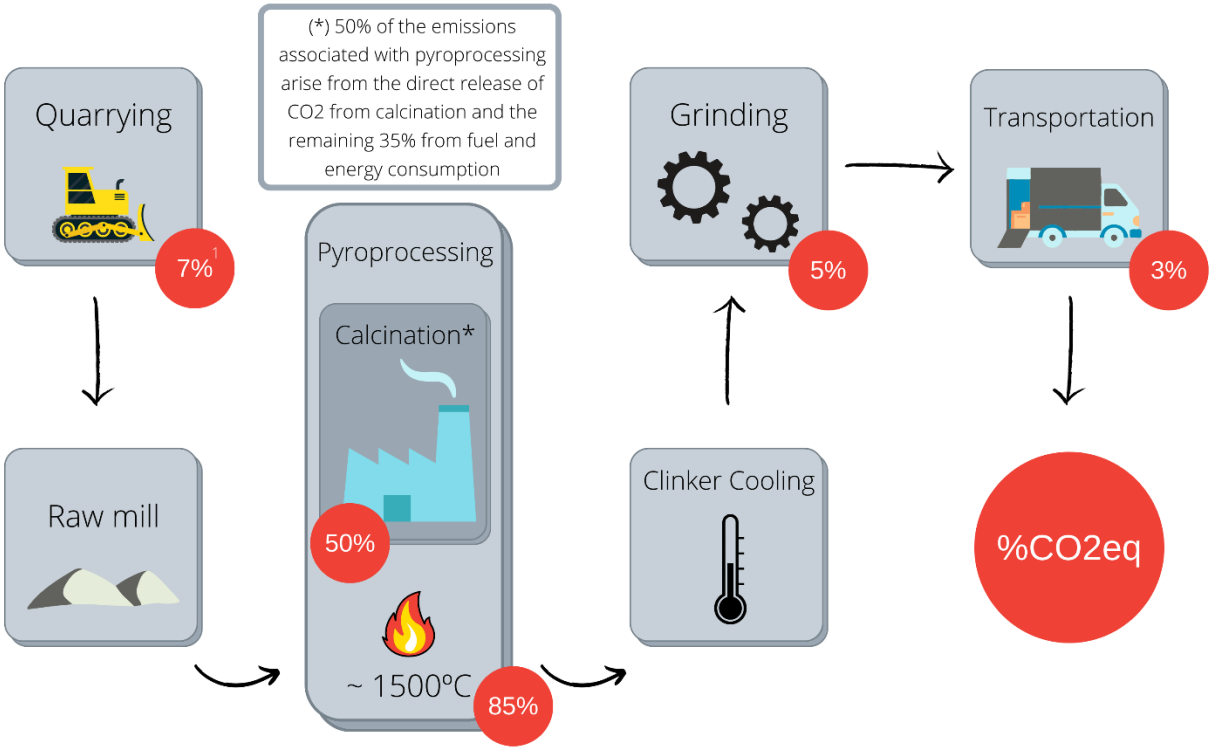

Figure 3: Simplified diagram of the cement production process (adapted)[16].
[1]Red circles indicate the percentage of CO_{2eq}(carbon dioxide equivalent) emissions associated with manufacturing.

The clinker can then be mixed with some pozzolans, such as volcanic ashes, calcinated clay, fly ash, and silica fumes, to produce the final Portland cement. That way, PC is considered a Calcium-Silicate-Hydrate (C-S-H) hydraulic cement and is the most common cement used today, with a composition of approximately 65% of calcium oxide, and the rest is generally a mixture of aluminum, iron and silica provenients from the clay and also limestone [13].

The hydration process of PC is indispensable to producing a stable, amorphous solid hydrate to be used in construction. This process requires clean water and involves a chemical reaction producing a solid phase that continues to grow and expand in the presence of water and cohesively encapsulates other materials inside the matrix of hydrate solid. It also produces heat. The reaction creates an alkaline substance (pH>12) due to the hydroxide (OH) ions produced, as described in equation 2[13,17].

$$Ca_3SiO_5 + 3H_2O \rightarrow 3Ca^{2+} + 4OH^- + H_2SiO_4^{2-} \qquad (2)$$

The importance of this process involves mainly the binding capacity of the hydraulic cement, which stems from the ability of new solid phases to precipitate from a supersaturated aqueous solution. This precipitation occurs in a manner that generates substantial solid-to-solid bonding interfaces within a previously liquid-filled volume[13]. As a result, hydraulic cement can be effectively utilized in construction applications as a fundamental component of concrete and mortar mixtures.

Mortars are artificial building materials mainly composed of three basic components: (i) inorganic binders, with the function of joining loose grains together through different chemical transformations in their mass; (ii) aggregates (or sands), which confer volume stability on the mortar mass during drying and enhance the mechanical resistance of the hardened mortar; (iii) water, which is necessary to mix all the mortar components into a viscous paste[18]. Adding more components, known as additives and admixtures, is possible to obtain some specific characteristics or properties.

A European Standard (EN 196-1) determines the composition of the mortar to obtain a reference value of compressive strength through tests and to evaluate the mechanical resistance of a cement mortar. This composition is three parts of sand to half part of water. In other words, it will have a certain amount of cement as the binder, three times this amount of sand and half of this cement amount of water (1:3:0,5)[19].

2.2. GEOPOLYMERS

Geopolymerization was described for the first time in the literature in the 1970s, when Joseph Davidovits, a French materials scientist, studied this reaction and its possible applications[20]. The result of this study is a product called geopolymer (GP), also commonly referred to as ‘low-temperature aluminosilicate glass’, ‘alkali-activated

cement', 'geocement', 'alkali-bonded ceramic', 'inorganic polymer concrete' and 'hydroceramic'[21].

According to Davidovits, there are hypotheses about using geopolymer binders when constructing ancient monuments (particularly Egyptian) over 4.000 years old[20]. He believes those people used the geopolymerization technique to build the constructions. Also, in history, Glukhovsky developed alkali-activated materials in the Soviet Union in the 1950s and 1960s. The researcher created alkaline systems by mixing volcanic materials with sodium hydroxide activating solutions[22]. In this way, they obtained hydrated calcium silicate phases (C-S-H), termed soil silicates. Followed by this, Davidovits developed a material using natural silicon and aluminum-rich materials, such as kaolin, reacted with alkaline liquid solutions.

Thus, a geopolymer is an aluminosilicate inorganic polymer with an amorphous three-dimensional network structure of silicon-oxygen tetrahedron $(SiO_4)^{4-}$ and aluminum-oxygen tetrahedron $(AlO_4)^{5-}$ connected through bridge oxygens (Figure 4). For the chemical designation of these geopolymers, Davitovits suggested the term poly(sialate), where sialate is an abbreviation for silicon-oxo-aluminate[20]. In other words, poly(sialate) is a giant molecular chain of silicon, oxygen, and aluminum.

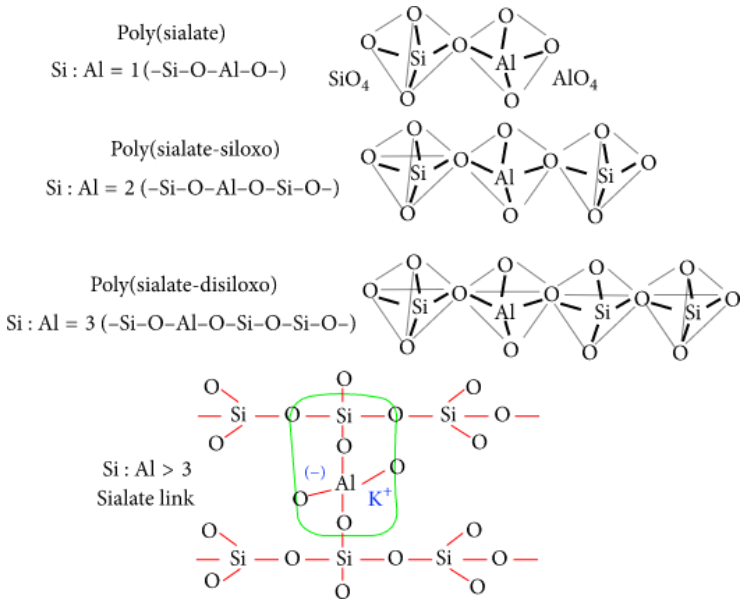

Figure 4: Three types of Polysialate[20].

As aluminum $(A1^{3+})$ and silicon (Si^{4+}) are in IV-fold coordination with oxygen (O^{2-}), the structure has a negative charge. That's why positive ions $(Na^+, K^+, Li^+, Ca^{2+}, Ba^{2+}, NH^{3+}\ H_3O^+)$ must be in the framework cavities to balance this charge. That way,

the reaction happens under the action of alkaline activators (such as KOH, NaOH, and Na_2SiO_3)[20,23,24]. Geopolymers are thus usually synthesized using alkaline silicate and hydroxide solutions to activate aluminate and silicate-rich materials, including natural minerals and industrial waste, such as metakaolin and fly ash[25].

It's important to point out that the term “alkali-activated materials (AAM)” is not used by Davidovits anymore; once AAMs are not polymers, they can’t be called geopolymers. According to him, they belong to two different and separate chemistry systems (a hydrate that is a monomer or a dimer versus an actual polymer)[26]. However, many scientists still use both terms as synonyms and publish studies with these nomenclatures, so it’s not unacceptable to portray it like an AMM and call the alkaline solution as an alkali activator.

These alkali activators are usually NaOH or KOH solutions and alkali metal silicate solutions, such as Na_2SiO_3 (sodium silicate), or a mixture of two alkali solutions[24]. The activation potential of the same concentration of activator is shown in equation 3[27]:

$$KOH < NaOH + Na_2CO_3 < NaOH < Na_2O \,.\, nSiO_2 \qquad (3)$$

A simplified chemical formula $M_n\{-(SiO_2)_z-AlO_2-\}_n$ was made to represent the geopolymer molecular structures without knowing the molecular details. The letter “M” is the alkali cation to balance the negatively charged $(Al(OH)_4)^-$, such as sodium (Na^+) or potassium (K^+). The subscript “z” defines the Si/Al molar ratio, which is an essential factor in determining the mechanical properties of the resulting geopolymers[25].

According to the description of Polysialates made by Davidovits, the Si/Al ratio can be 1, 2, or 3[20]. But there are a lot of updated works that show a ratio higher than three[28]. Ahmari and Zhang[29] have produced eco-friendly bricks for construction using copper mine tailings, which contain 64,8 wt% of SiO_2 and 7,08 wt% of Al_2O_3 (Si/Al ratio around 8:1). Also, in literature, different Si/Al ratios have been reported to obtain the maximum compressive strength of geopolymers. For example, Duxson et al. [30] reported a maximum strength at Si/Al ratio of 1,9 from metakaolin-based geopolymers; however, Silva et al.[31] stated that of 1,7 from metakaolin/sodium silicate/sodium hydroxide geopolymer. And Rowles and O' Connor[32] even reported that the maximum strength was 64 MPa at a Si/Al/Na ratio of 2,5:1:1.3 in synthesizing a metakaolin-based geopolymer with sodium silicate as an activator.

Therefore, the choice of this ratio will influence the material properties and, consequently, the applications. Davidovits found some possible applications of geopolymers in industries such as construction, aerospace, and plastic. The classification application of geopolymer material based on the Si:Al ratio is presented in Table 1[33].

Table 1: Applications of geopolymer materials based on Si:Al ratio (adapted)[33].

Si:Al ratio	Applications
1	Bricks
	Ceramic
	Fire Protection
2	Cement and concrete
	Toxic waste management
3	Fire protection fibre glass composite
	Heat-resistant composite (200 °C-1000 °C)
> 3	Sealants for industry (200 °C-600 °C)
20 - 35	Fire resistant and heat resistant fibre composites

Now, regarding the geopolymerization process, it consists of dissolution and reorganization, condensation and polymerization (Figure 5):

Dissolution - Under the action of alkali, the aluminosilicate precursor hydrolyzed has the silicon-oxygen bond and aluminum-oxygen bond broken to form several types of oligomers;

Reorganization - Silicate, aluminate, and aluminosilicate together constituted the transition phase after hydrolysis;

Condensation - Oligomers start to connect by a condensation reaction and form a small network structure under strong alkali conditions;

Polymerization - Geopolymer substances are connected to form a three-dimensional network structure. Then, a dense and complex geopolymer material is formed after further dehydration and condensation[8,24].

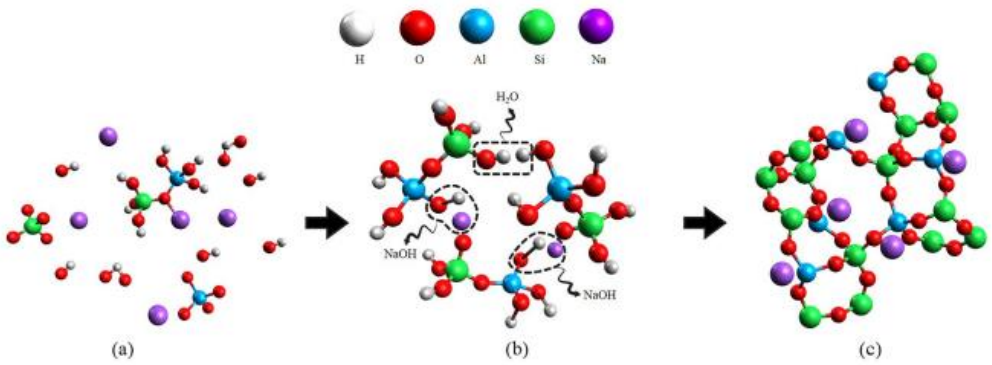

Figure 5: Schematic illustration of the geopolymerization process. a) reorganization of aluminosilicate. b) gel formation from oligomers condensation. c) polymerization[8].

In experimental works, based on the determination of the ratios previously mentioned, the fresh geopolymer starts the curing process by mixing all the geopolymer components. In the literature, there are some specific techniques to do this cure once the temperature and time influence the properties of the final material[34]. For example, curing temperature is crucial for achieving higher strength for alkaline activated fly ash. Specimens subjected to higher curing temperatures exhibited higher mechanical strength than those at lower temperatures. The longer duration of curing also results in better strength, but the increase of strength is negligible when curing time is extended beyond 24 hours[35,36]. So, what was observed in most of the studies, is that for an efficient geopolymerization, the curing temperatures should be between 40 °C to 85 °C and around 24 to 48 hours[34].

2.2.1. Geopolymer precursors

Geopolymers are synthesized by mixing source materials containing alumino-silicate with alkaline solutions. Source materials may be kaolinite, clays, zeolite, fly ash, silica fume, slag, palm oil fuel ash, rice-husk ash, and red mud, among others, and some of them with a pre-treatment[37].

Table 2 shows some studies about the most used precursors and the properties of the resultant geopolymers. Most of these precursors are solid wastes already used for commercial purposes. For example, the Australian company “Wagners” use blast furnace slag (waste from iron production) and fly ash (waste from coal-fired power generation) as precursors[38] to produce geopolymeric concrete, which finds applications in the construction industry.

Table 2: Geopolymer precursors reported in the literature.

Author	Precursor	Geopolymer properties
Gao et al.[39]	Kaolinite	Porous material with thermal and sound insulation
Singh et al.[40]	Red mud	Good dry compressive strength
Rattanasak et al.[41]	Fly ash	Good compressive strength
Liew et al.[42]	Clay	Good chemical, fire and thermal resistance
Chindaprasirt et al.[43]	Bottom ash	Medium compressive strength
Cheng and Chiu[44]	Granulated blast furnace slag	Good fire resistance
Villa et al.[45]	Natural zeolite	Good compressive strength
Pimraksa et al.[46]	Diatomaceous Earth	Lightness

2.2.1.1. Solid wastes as precursors

As mentioned previously, to produce a geopolymer, an aluminosilicate material is necessary to be the precursor of the reaction. This material is not difficult to find since aluminosilicate minerals are among the most abundant in the earth's crust. Moreover, solid wastes have been used as a source of aluminum, silicate, or both, to act as precursors in the production of geopolymers[24].

An enormous amount of solid waste is produced yearly from various human activities, such as mining, iron and steel metallurgy, power generation, manufacturing industry, agricultural production, and electronic products. This waste can cause damage to human beings and the ecological environment, like the occupation of areas of valuable land and pollution of water, soil, and atmosphere, triggering severe environmental problems during the accumulation process[24,47,48].

According to the Chinese National Annual Report of Solid Waste Pollution Prevention and Control in Big and Medium-Sized Cities, in 2018, China's cities generated 1.55 billion tons of general industrial solid waste and industrial hazardous waste reached 46.4 million tons, and the amount of municipal solid waste was 21.1 million tons[24,49]. Therefore, it is essential to reuse or recycle this waste into building materials, roadbed materials, and soil conditioners, acting for a circular economy.

According to Morseletto P.[50], the circular economy (CE) is "an economic model aimed at the efficient use of resources through waste minimization, longterm value retention, reduction of primary resources, and closed loops of products, product parts, and materials within the boundaries of environmental protection and socio-economic

benefits." So, a circular economy aims to minimize the use of non-renewable resources and waste production while reusing and recycling dominate the life cycles of materials[51,52]. Using solid wastes as precursors in geopolymers is one crucial example in this context.

The most recent literature exposes some different precursors and the benefits of each in the geopolymers produced, as shown in Table 2. Several solid wastes have distinctly different results on the structure and properties of geopolymer materials, thus affecting specific applications[24,47]. These wastes are divided into several categories (Figure 6). Some solid waste examples are silica fume (SF), fly ash (FA), metakaolin (MK), red mud (RM), waste glass, copper mine tailings, rice husk ash (RHA), and diatomaceous earth (DE), among others.

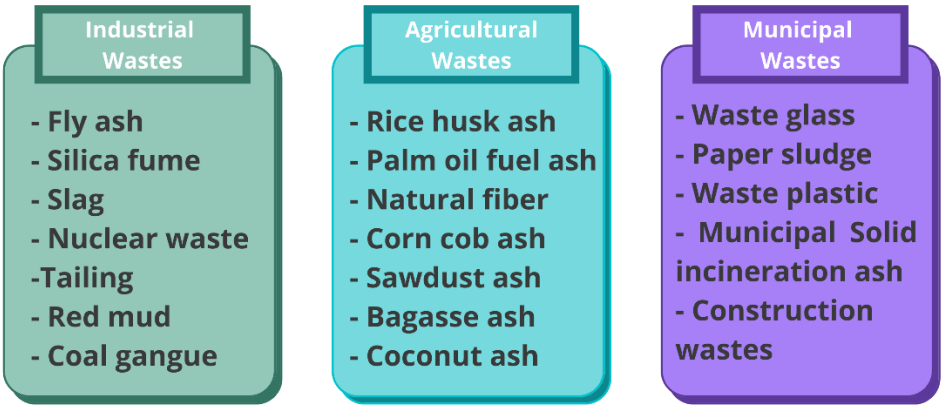

Figure 6: Categories of solid wastes used in the production of geopolymers (adapted)[24].

The properties and structure of the geopolymers will thus depend on raw material characteristics, such as Si/Al ratio, particle size range, phase composition, and amorphous content[24]. Table 3 presents the chemical composition of some solid wastes previously mentioned that can be used in GP. It's important to note that it is common to synthesize geopolymers with more than one raw material to obtain a better source of aluminum and silicon, like fly ash with slag, fly ash with red mud, and diatomaceous earth with alumina.

Table 3: Chemical composition of solid wastes used in the production of geopolymers (adapted) [24,53–65].

Solid wastes	Elements (%)										
	SiO_2	Al_2O_3	Fe_2O_3	CaO	Na_2O	MgO	MnO	K_2O	SO_3	LOI	Total
Low calcium fly ash	60.57	21.35	4.17	2.01	0.68	0.75	--	1.40	--	3.29	94.22
High calcium fly ash	34.80	7.68	6.91	30.68	0.64	1.18	--	0.27	10.55	--	92.71
Silica fume	95.72	0.09	0.63	0.23	0.09	0.37	0.02	0.26	0.01	2.53	99.95
Red mud	12.83	20.26	33.39	0.87	10.85	0.00	--	--	0.60	12.28	91.08
Blast furnace slag	35.95	10.01	1.48	33.07	1.39	6.43	3.44	0.74	3.52	--	96.03
Vanadium tailing	61.91	7.35	4.12	6.51	2.66	1.24	--	1.25	7.14	6.93	99.11
Iron ore tailing	34.74	16.22	12.31	7.63	0.54	8.92	0.13	1.52	--	13.18	95.19
Quartz mill tailing	97.47	1.10	0.3	0.17	0.04	0.21	--	0.02	--	0.71	100.00
Rice husk ash	93.1	0.3	0.2	1.5	0.06	0.6	--	2.3	--	0.8	98.86
Palm oil fuel ash	64.20	4.25	3.13	10.20	0.10	5.90	--	8.64	0.09	1.73	98.24
Biomass ash	25.34	6.05	4.15	36.72	0.95	3.61	0.42	5.84	3.84	--	86.92
Municipal solid incineration ash	10.22	4.18	--	38.58	8.07	--	4.95	6.02	5.26	--	77.28
Waste glass	70.5	3.2	0.42	10	12	2.3	--	1.0	--	--	99.42

2.2.1.2. Diatomaceous earth

Diatomaceous earth (DE) is almost pure amorphous silicon dioxide, made up of fossilized diatoms, a significant group of algae, the most common types of phytoplankton, and probably the most widespread group of plants on the earth. These diatom species are primarily unicellular and characterized by an external skeleton (frustule) rich in silicon dioxide whose fossilized remains constitute DEs[66–68].

DE is used extensively and is prepared for commercial use by quarrying, drying and milling[66]. Mainly in the Eocene and Miocene epochs, i.e., around 20 to 80 million years ago, different species of diatoms extracted silicon from water, producing a hydrated amorphous silica skeleton. When the diatoms died, the tiny shells sunk and formed thick layers over the centuries. After a long time, these deposits were fossilized and compressed into a soft and chalky rock called diatomite or diatomaceous earth. Deposits range in thickness from a few centimeters to several hundred meters, and they may be compact or finely laminated.

As mined, DE contains 50% or more moisture. Around 86 to 94% of the solids are silica; the rest is mainly alumina and alkalies from clay. The only change to

diatomaceous earth during processing is the reduction in the moisture content and mean aggregate particle size. Moisture is reduced to 2-6%, and milling reduces particle size to between 0.5 and 100 µm, with the majority between 10 and 50 µm. This process results in a fine, talc-like powder or dust considered non-toxic to humans and animals when inhaled[66]., and it's known by commercial DE.

For some applications, such as filtering, this commercial diatomaceous earth is calcined at a temperature above 1000 ºC, which turns the amorphous silica into crystalline silica. However, when inhaled, this crystalline silica can be toxic to humans and animals, so calcined diatomaceous earth is not used for animal feed and is not food grade[69,70].

Some application examples of calcined DE are its use for water purification, clarifying liquors and juices, filtration of commercial fluids, and separating various oils and chemicals[71]. In the wine industry, diatomaceous earth has been used as a filtration adjuvant due to the extreme porosity of the powder obtained by processing the rock. e diatomaceous earth is continuously added to the turbid wine before it enters the filter. The filter layer grows thicker throughout the process, the impurities are distributed through the mass, and the outside layer is never blocked[72]. This process, called "earth filtration," has been used to clarify wines.

In Table 4, it is possible to observe that a significant amount of adjuvant is necessary for this filtration process. After use, diatomaceous earth loses its filtering capacity; it becomes a residue with toxic properties to the environment[69,70]. So, one disadvantage is that it involves discharging large volumes of spent diatomaceous earth (SDE) that represent a source of environmental pollution[72].

Table 4: Precoat filtration - quantity and quality of adjuvants required to treat different products (adapted)[72].

Products to be filtered	First, precoat (time: 10 - 20 min)		Second precoat (time: 10 - 20 min)		Continuous Accretion		Flow rate ($hl/h/m^2$)
	Quality (Darcy)	Quantity (kg/m^2)	Quality (Darcy)	Quantity (kg/m^2)	Quality (Darcy)	Quantity (kg/hl)	
New wine, first filtration (December)	2 - 3	0.5 - 1	2 - 3	0.5	2 - 3	200 - 300	5
Press wine	2 - 3	0.5 - 1	2 - 3	0.5	2 - 3	200 - 400	5
Wine aged for at least one winter	1 - 2	0.5	1 - 2	0.5	1 - 2	50 – 200	10
Wine sheet or lenticular module filtered before bottling	1	0.5	0.4 - 1	0.5	0.4 - 1	20 – 50	15
Wine membrane filtered before bottling	1	0.5	0.06 - 0.4	0.5	0.06 - 0.4	20 – 50	15

To avoid the waste of SDE, scientists are studying its use as a source of silica to act as a precursor in the production of geopolymers, with good results being obtained. Some used SDE as a precursor in mixtures with calcium aluminate cement[73], and others studied the combination of RHA and diatomaceous earth in lightweight geopolymer manufacture[74]. Mejia et al. used diatomite as a source of silica in activating solution, which was used to activate a mixture of metakaolin and fly ash, with mortars of up to 38 MPa in developed strength[75]. Font et al. also used spent diatomaceous earth to produce geopolymers and made a comparison with commercial diatomaceous earth. The results showed that after 28 days of cure, SDE samples obtained similar and even better (calcinated SDE) mechanical results than the commercial samples[76].

2.3. GEOPOLYMERS IN MORTARS

The production of mortars with alternative binders, such as geopolymers, is becoming more common to reduce the harmful effects of cement production. Some scientific works exemplify the composition, production, cure, and properties of geopolymeric mortars, as presented in Table 5.

Table 5: Some recent research works on geopolymeric mortars.

Author	Precursor	Activator	Geopolymeric mortar properties
Albitar et al.[77]	FA and GLSS	NaOH and Na_2SiO_3	High durability
Castel and Foster[78]	FA and GGBFS	NaOH and Na_2SiO_3	High early bond strength
Zhang et al.[79]	MK and FA	K_2SiO_3 and KOH	High-temperature resistance
Huseien et al.[80]	MK	NaOH and Na_2SiO_3	Good workability
Phoo-ngernkham et al.[81]	FA and GBFS	NaOH and Na_2SiO_3	High compressive strength
Hawa et al.[82]	MK and OPA	NaOH and Na_2SiO_3	High compressive strength
Karim et al.[83]	GBFS, POFA and RHA	NaOH	Thermal resistance
Miranda et al.[84]	FA	NaOH and Na_2SiO_3	Corrosion resistance
El-Sayed et al.[85]	GBFS	NaOH and Na_2SiO_3	Sulfate resistance
Prabu et al.[86]	RHA and FA	NaOH, KOH, K_2SiO_3, and Na_2SiO_3	Acid resistance
Revathy V. [87]	FA	NaOH	High compressive strength

Revathy V.[87] compared the strength of geopolymer mortar and cement mortar. He used fly ash as the precursor, and the alkaline solution was made of sodium hydroxide and sodium silicate. The concentrations of NaOH used were 10, 12, and 15M. The geopolymer mortars were cured at ambient conditions for 28 days, while the cement mortars were placed in a curing chamber at 25 ºC and 100% relative humidity. The compressive test results showed that both materials had similar compressive strengths in 28 days (Figure 7).

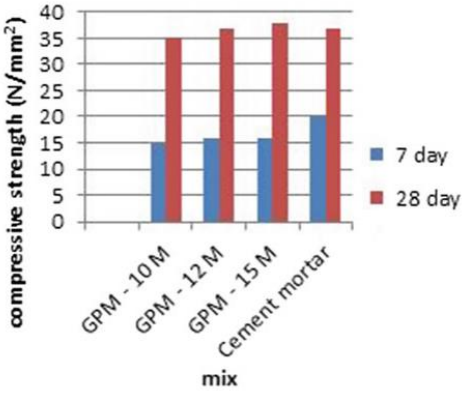

Figure 7: Compressive strength of geopolymers (GPM) and cement mortars[87].

Geopolymer composites, especially with MK and FA, provide the significant advantages of superior durability[77], bond behavior[78], and high-temperature resistance[88], compared to cement composites. Zhang P.[79,89] produced a metakaolin/fly-ash-based geopolymer. From that, the scientist used MK and FA as precursors, with a proportion of 70 and 30%, respectively, and in some samples, nano silicate (NS) was added to obtain better workability and Polyvinyl Acetate (PVA) fiber to improve the strength properties.

The activating solution was sodium silicate and sodium hydroxide solution with a 6,3:1 mass ratio, and the water-binder mass ratio was 0,65, already considering the water in the other substances. A superplasticizer was also used in the composition. Table 6 is shown the mix design of this work.

Table 6: Mix designs for the samples prepared by Zhang P. (adapted)[89].

MK (kg/m^3)	FA (kg/m^3)	Water (kg/m^3)	Na_2SiO_3 (kg/m^3)	NaOH (kg/m^3)	Quartz sand (kg/m^3)	PVA fiber (%)	Nano-SiO_2 (%)	Superplasticizer (kg/m^3)
429.5	184.1	106.2	445.4	71	613.6	0	0	3.07
429.5	184.1	106.2	445.4	71	613.6	0.2	0	3.07
429.5	184.1	106.2	445.4	71	613.6	0.4	0	3.07
429.5	184.1	106.2	445.4	71	613.6	0.6	0	3.07
429.5	184.1	106.2	445.4	71	613.6	0.8	0	3.07
429.5	184.1	106.2	445.4	71	613.6	1.0	0	3.07
429.5	184.1	106.2	445.4	71	613.6	1.2	0	3.07
425	182.2	106.2	445.4	71	613.6	0	1.0	3.07
425	182.2	106.2	445.4	71	613.6	0.2	1.0	3.07
425	182.2	106.2	445.4	71	613.6	0.4	1.0	3.07
425	182.2	106.2	445.4	71	613.6	0.6	1.0	3.07
425	182.2	106.2	445.4	71	613.6	0.8	1.0	3.07
425	182.2	106.2	445.4	71	613.6	1.0	1.0	3.07
425	182.2	106.2	445.4	71	613.6	1.2	1.0	3.07

For the preparation of the mortars, the author first mixed the solid materials (MK, FA, and Sand). Then, mixed the alkaline solution ($NaSiO_3$ and NaOH) and added it into the solid mix. After that, water, NS and superplasticizer were putted on and finally the PVA fiber was also added. Figure 8 shows this procedure.

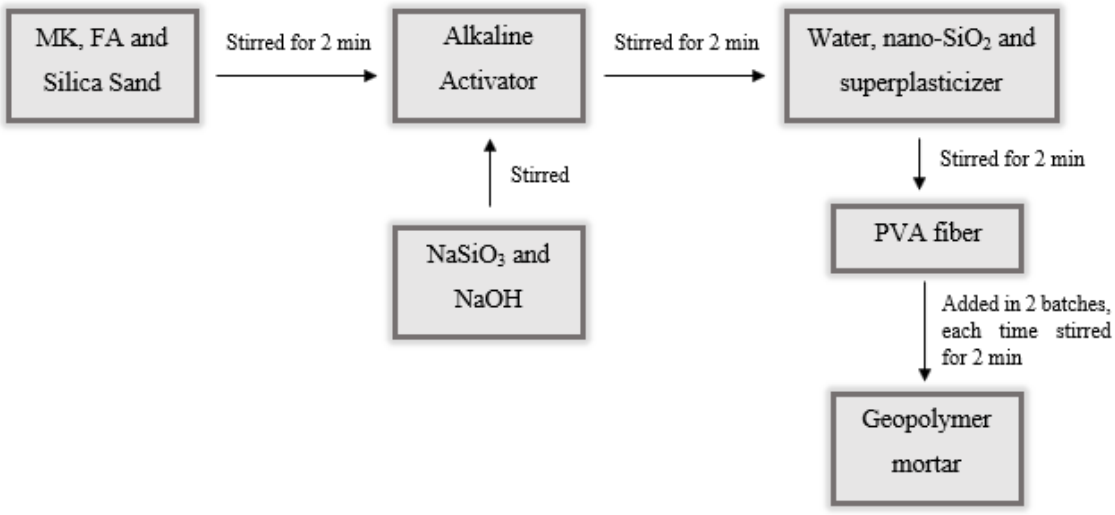

Figure 8: Process of preparation of geopolymer mortars (adapted)[89].

Then, a compressive strength test showed a compressive resistance to the basic geopolymer mortar sample (without PVA and NS) of around 45 MPa. The resistance was even higher in the samples with PVA and NS (Figure 9).

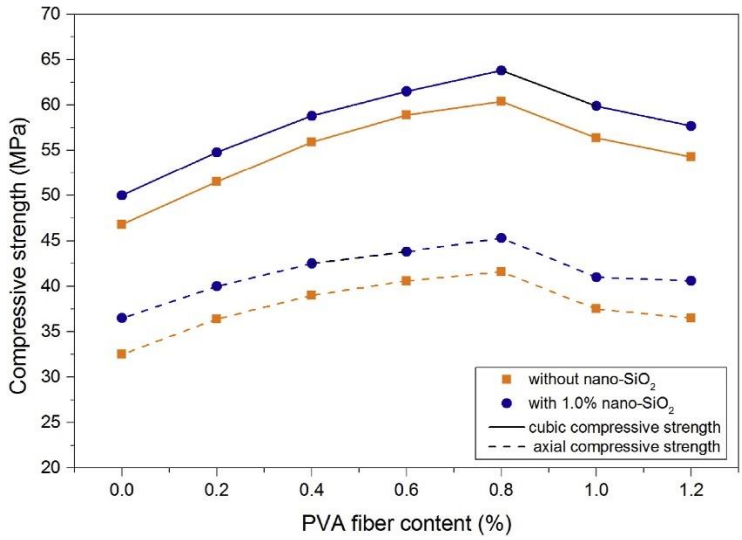

Figure 9: Compressive strength with different PVA fiber fractions[89].

Pacheco-Torgal F.[90] has studied alkali-activated metakaolin-based mortars and several factors influencing workability and mechanical strength. He used MK as the precursor, with a previous thermal treatment at 650 ºC for a few seconds using a flash calcination apparatus. In some samples, the author substituted MK with calcium hydroxide. The activating solution was sodium hydroxide solution varying the concentration in 10, 12, 14, and 16M and sodium silicate in a mass ratio of 1:2,5. This ratio was used because previous investigations showed that this ratio leads to the highest compressive strength results in alkali-activated mortars.

The mass ratio of sand/metakaolin/activator used was 2.2/1/1 because, in previous trials, a higher sand content led to a very stiff behavior, and a lower one led to liquid-like mortar. A superplasticizer was also used in the composition. The mixing process involved a dry mix of sand and metakaolin, and the activator was added. The curing process was at 20 ºC for 24 hours in the mold and then outside the mold until the mechanical test day.

The compressive strength was analyzed within 7 days of cure, and the workability was analyzed according to a flow test to understand the NaOH concentration's influence.

Figure 10 shows some results.

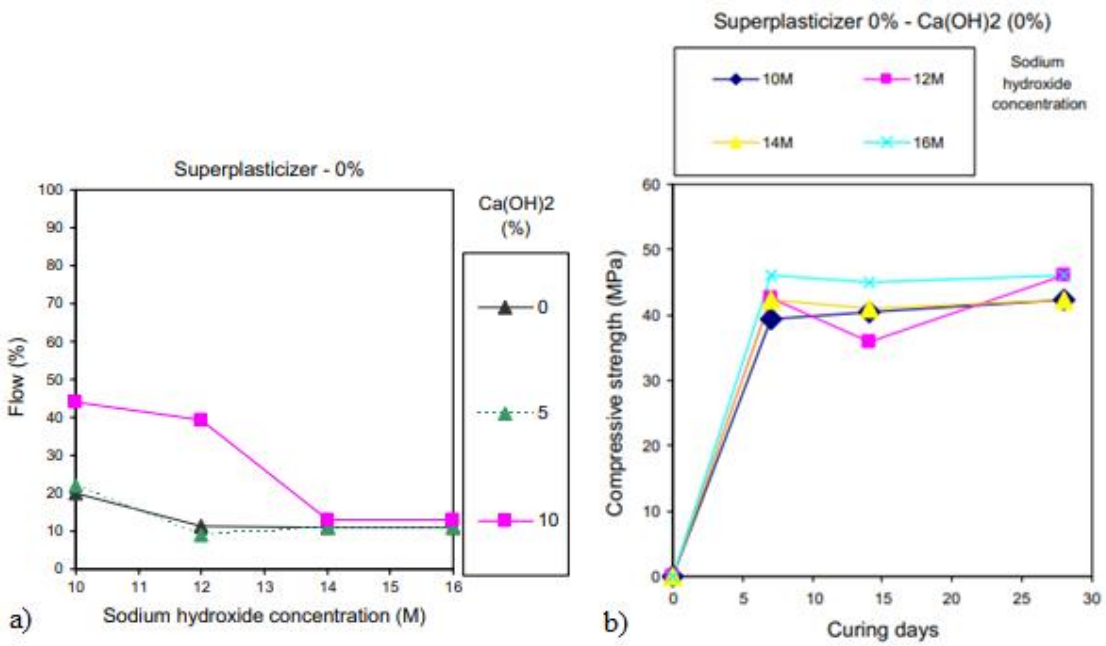

Figure 10: Results of Pacheco-Torgal F. study. a) Flow versus sodium hydroxide concentration for several contents of calcium hydroxide. b) Compressive strength according to age for mortar mixtures with different sodium hydroxide concentrations[90].

The results show that the mortar's workability is reduced with the increased sodium hydroxide concentration and that the compressive strength increased by around 35% with sodium hydroxide concentration.

2.3.1. Diatomaceous earth in geopolymeric mortars

There are not many studies addressing the application of diatomaceous earth as precursor of geopolymers applied specifically to mortars, but Villca A.[91] produced a geopolymeric mortar with lime-pozzolan mixture, rice husk ash (RHA) and spent fluid catalytic cracking (FCC) as precursors and, for the activating solution, it was used sodium silicate, sodium hydroxide, RHA and residual diatomaceous earth (RDE), or spent diatomaceous earth, from the beer industry. These were used as alternative silica sources with a lower carbon footprint. All mortars were produced at set sand:binder ratio of 3.

The binder in the traditional mortars produced for this study (containing only lime and pozzolan) is the sum of lime and pozzolan. For hybrid mortars, the binder is composed of 30 wt.% of FCC (precursor of the geopolymeric binder), and 70 wt.% of the binder is used for traditional mortars (lime–pozzolan mixture).

All the activating solutions were prepared at a SiO_2/Na_2O molar ratio of 1,17, a water:binder ratio of 0,6, and 1,69 mol of Na_2O per kg of precursor[91,92]. Otherwise, the lime–pozzolan proportions employed for the traditional mortars were set according to previously performed studies: a water:binder ratio of 0,8, and a lime/pozzolan proportion of 1:1 for lime:FCC and one of 1:2 for lime:RHA[91,93]. In Table 7, the mix proportions are detailed.

Table 7: Mix proportions of traditional and hybrids mortars (adapted)[91].

	Lime-Pozzolan Binder				Geopolymeric Binder				Sand
					Alkaline-Activating Solution				
	Lime	Pozzolan	H_2O	FCC	H_2O	NaOH	Na_2SiO_3	RHA or RDE	
T-FCC	262.5	262.5	420.0	-	-	-	-	-	1575.0
H-FCC/C	183.8	183.8	294.0	157.5	37.8	19.2	88.6	-	1575.0
H-FCC/RHA	183.8	183.8	294.0	157.5	94.5	37.8	-	27.6	1575.0
H-FCC/RDE	183.8	183.8	294.0	157.5	94.5	37.8	-	27.6	1575.0
T-RHA	175	350.0	420.0	-	-	-	-	-	1575.0
H-RHA/C	122.5	245.0	294.0	157.5	37.8	19.2	88.6	-	1575.0
H-RHA/RHA	122.5	245.0	294.0	157.5	94.5	37.8	-	27.6	1575.0
H-RHA/RDE	122.5	245.0	294.0	157.5	94.5	37.8	-	27.6	1575.0

The nomenclature “T-X” represents the traditional mixtures based on lime–pozzolan, where “T” indicates a traditional mixture and “X” is related to the used pozzolan: “FCC” or “RHA.” The nomenclature “H-X/Y” was adopted to represent hybrid systems, where “H” indicates hybrid systems, “X” is related to the pozzolan used in the previously explained traditional mixture (lime–pozzolan), and “Y” denotes the type of alkaline-activating solution: “C” stands for commercial solution (NaOH and Na_2SiO_3), “RHA” for an alternative solution using RHA as the alternative silica source and “RDE” for an alternative solution employing RDE as an alternative silica source.

Besides that, geopolymers with similar proportions (without sand) and cured under the same conditions were prepared according to the microstructural analysis.

Experimental tests were further performed to measure the compressive strength of the mortars with 3, 7, 28, and 90 curing days. The results obtained are presented in Figure 11.

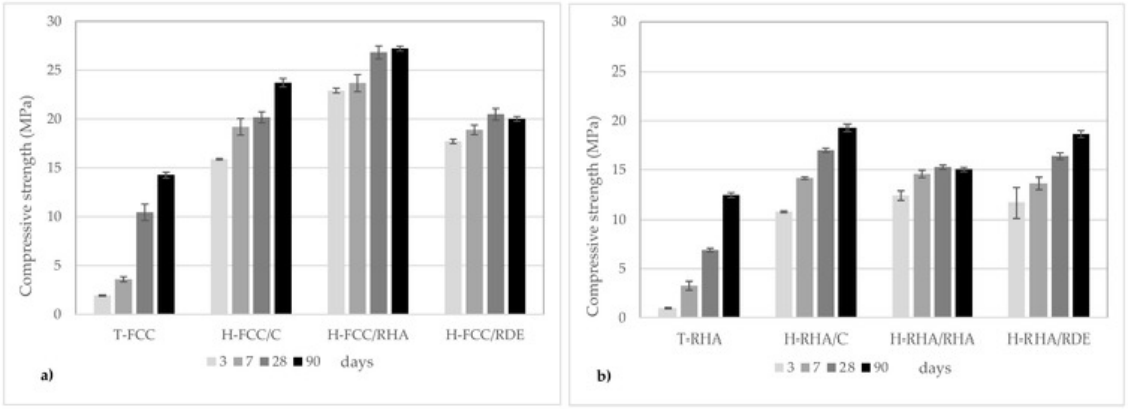

Figure 11: Compressive strength of mortars after 3, 7, 28, and 90 days of curing. a) FCC systems. b) RHA systems[91].

The results of hybrid systems versus traditional mixtures were positive. After 3 days of curing, all hybrid mixtures showed similar or even higher compressive strength values than traditional mixtures after 90 days, regardless of the employed pozzolan type. Moreover, the hybrid mortars prepared using Residual Diatomaceous Earth as an alternative silica source yielded a similar compressive strength to the hybrid systems using commercial reagents for 3–28 days of cure. These results are fascinating from an environmental point of view because of the high carbon footprint associated with other activating solutions[91,94].

3. OBJECTIVES

3.1.1. General Objective

This work's main objectives are preparing geopolymers from spent diatomaceous earth (SDE), preparing mortars with these geopolymers, evaluating their performance in mechanical characterization, and comparing the produced geopolymer and geopolymeric mortars with the literature.

3.1.2. Specific Objectives

The specific objectives of this research are to:

I. Characterize the SDE;
II. Determine the best production methodology for geopolymers based on the literature;
III. Prepare geopolymers using SDE as a precursor;
IV. Characterize the geopolymers through XRD, FTIR, BET, and SEM/EDS;
V. Prepare geopolymeric mortars by combining a geopolymer binder with Portland cement in a particular proportion;
VI. Characterize the mortars by compressive and flexural tests and flow test;
VII. Compare results according to the literature.

4. MATERIALS AND METHODS

4.1. MATERIALS

The reactants used in this work are described below.

- Spent diatomaceous earth provided by Caves Campelo;
- Aluminum oxide (Al_2O_3 - 99,7% pure) provided by Thermo Scientific;
- Sodium hydroxide (NaOH - pearls 1-2 mm) provided by Labkem;
- Sodium silicate solution ($H_{10}Na_2O_8Si$ - Na_2O = 10.6% and SiO_2 = 26.5% - 1,5 S.G.) provided by Fisher Scientific;
- Standard sand (EN 196-1) provided by Societe Nouvelle du Littoral;
- Portland Cement (32,5N) provided by Secil;
- Distilled water.

4.2. METHODS

The study, based on experimental research, of the synthesis of geopolymer and geopolymeric mortar based on diatomaceous earth was conducted in five stages: pre-treatment of the SDE, its characterization, synthesis, and characterization of the geopolymer, synthesis, and characterization of the geopolymeric mortar and analysis of the obtained results.

The produced geopolymers used alkaline solutions based on sodium hydroxide of 10 M and 12 M and sodium silicate (SS). Si/Al ratios of 2,5 and 3,5 were chosen to follow the literature. The samples were cured for four days in an oven at 40 ºC and then at room temperature. The geopolymer composition was chosen after the characterization of the SDE used as a precursor. Finally, the influence of the alkaline solution concentration and the Si/Al ratio was evaluated.

The geopolymeric mortars were produced using fresh geopolymer with the same composition used previously as part of the binder. This binder was composed of different percentages of cement and geopolymer. In the final work, mortars with 75%, 90% and 100% of geopolymer in the binder were analyzed, with the remaining percentage of 75% and 90% samples being cement.

The research was carried out at the Mountain Research Centre – CIMO, Laboratory of Analytical Chemistry, Laboratory of Structures and Strength of Materials, and Laboratory of Construction Materials at the Polytechnic Institute of Bragança. Some analyses were performed at Rey Juan Carlos University and at The University of Trás-os-Montes and Alto Douro.

The physical and chemical tests and analyses carried out on the material followed the criteria of the laboratories in which they were performed and were also based on the consulted bibliographies. The research steps are shown in the flowchart in Figure 12.

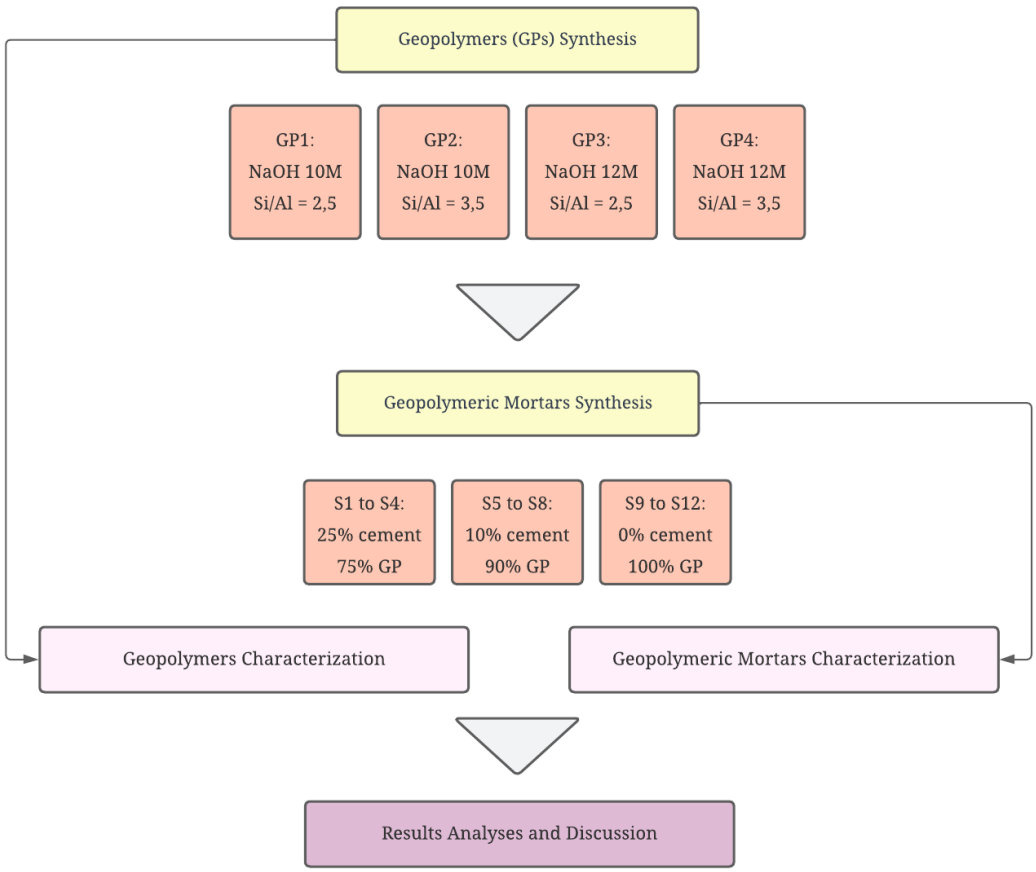

Figure 12: Flowsheet of Methodology Stages.

Then, the five stages mentioned above are described in detail in the sections below.

4.2.1. Pre-treatment of the spent diatomaceous earth

The SDE, after disposal, still has some winery wastewater in its composition, as Figure 13a shows. This way, the samples received were dried at room temperature before

further processing. After that, they were calcined in a furnace for 2,5 hours at 700 ºC. The result is shown in Figure 13b.

Figure 13: Spent diatomaceous earth. a) Before calcination. The red sample is from red wine filtration, and the beige is from white wine filtration. b) After calcination.

The calcination process is necessary to ensure the removal of volatile compounds, oxidize organic matter and remove unwanted impurities from the SDE. This way, temperatures around 700 ºC can eliminate an amount of this organic material, which was determined by an ash content analysis.

4.2.2. Determination of Calcinated Spent Diatomaceous Earth's Characterization

After the pre-treatment of the SDE, the sample was analyzed by inductively coupled plasma-optical emission spectrometry (ICP-OES), Fourier-transformed infrared spectroscopy (FTIR), X-ray diffraction (XRD), Scanning Electron Microscopy with Energy Dispersive X-ray Spectroscopy (SEM-EDS) and Surface and Pore Analyzer.

ICP-OES was performed to determine the elemental composition of the samples[95]. This analysis was necessary to determine the geopolymer formulation and was performed in triplicate by ICP-OES spectrometer (Thermo Fisher Scientific ICAP 7400 duo). The lead was analyzed on 220.353 nm wavelength.

FTIR analyses were performed to obtain information about the chemical structure of the SDE[96]. In this work, the FTIR spectra of the diatomaceous earth were recorded on a Perkin Elmer FT-IR spectrophotometer UATR Two infrared spectrophotometer, with a resolution of 4 cm^{-1}. The range of wavenumber used in the analysis was from 450 to 4000 cm^{-1}. The measurement was done from the solid sample at room temperature.

XRD analyses were performed to examine the material properties such as phase composition and structure[97]. These analyses were performed in a PANalyticalX'Pert PRO equipped with a X'Celerator detector and secondary monochromator (Cu Kα λ = 0.154 nm; data recorded at a 0.017◦ step size).

SEM/EDS analysis is a highly versatile tool that can examine and analyze the microstructural properties of solid objects. Its usefulness is primarily attributed to the exceptional level of resolution that it can provide when examining bulk objects, with values as small as 10 nm being achievable. Additionally, SEM images offer a three-dimensional representation of the specimen due to its significant depth of focus[98]. The samples analyzed in this study were collected in powder form and were examined at scales of 100, 20, and 10 μm.

The properties of the materials' texture were analyzed using N_2 adsorption-desorption isotherms at 77 K. These isotherms were obtained using a Quantachrome instrument NOVA TOUCH LX[4], which utilized long cells with a bulb and an outer diameter of 9 mm. To prepare the samples, a method of outgassing was employed at 120°C for 16 hours, as recommended by IUPAC. The specific surface area (S_{BET}) was determined by applying the BET method, and the average pore radius and the pore volume by applying the Barrett-Joyner-Halenda (BJH) method with Quantachrome TouchWin software, which analyzed the data in the range of p/p_0 0.05 – 0.99

IUPAC has developed a revised system for categorizing physisorption isotherms. This updated classification, depicted in Figure 14, represents the most recent proposal from IUPAC[99]. With these classifications of the isotherms obtained, it is possible to characterize the diatomaceous earth in terms of the type of material.

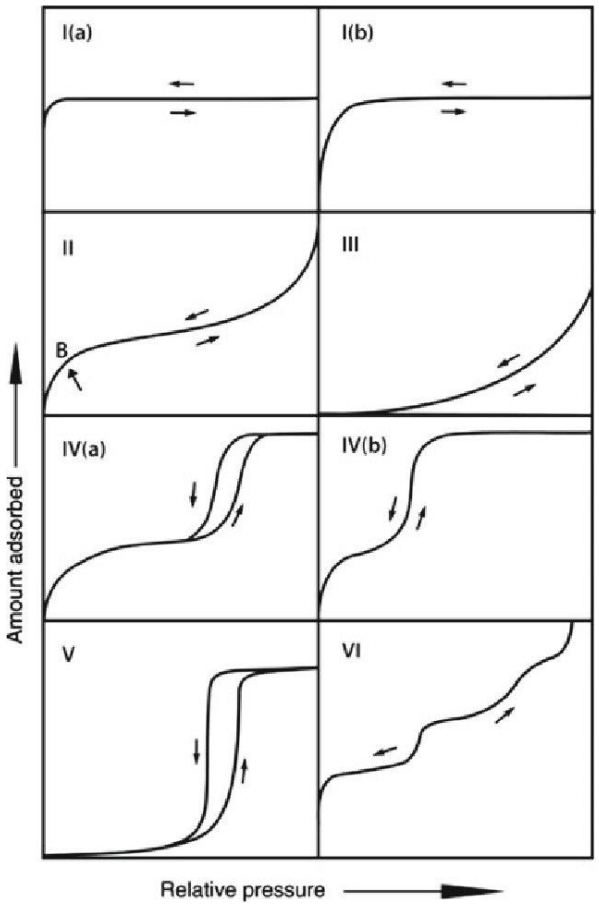

Figure 14: Classification of physisorption isotherms by IUPAC [99].

4.2.3. Determination of Geopolymers Synthesis and Characterization

4.2.3.1. Geopolymers Synthesis

The geopolymer was produced as shown in Figure 15, Figure 16, and Figure 17.

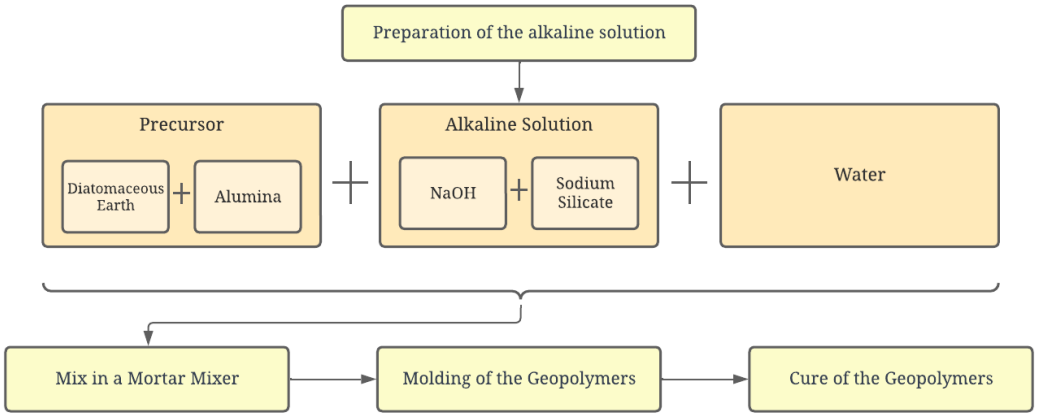

Figure 15: Flowchart of Geopolymers Production.

First of all, the alkaline solution was prepared by mixing sodium hydroxide solution with SS for 10 minutes in a magnetic stirrer. Later, as shown in Figure 16, the

SDE (1) and the aluminum oxide (2) were mixed (3) until a homogeneous powder was obtained.

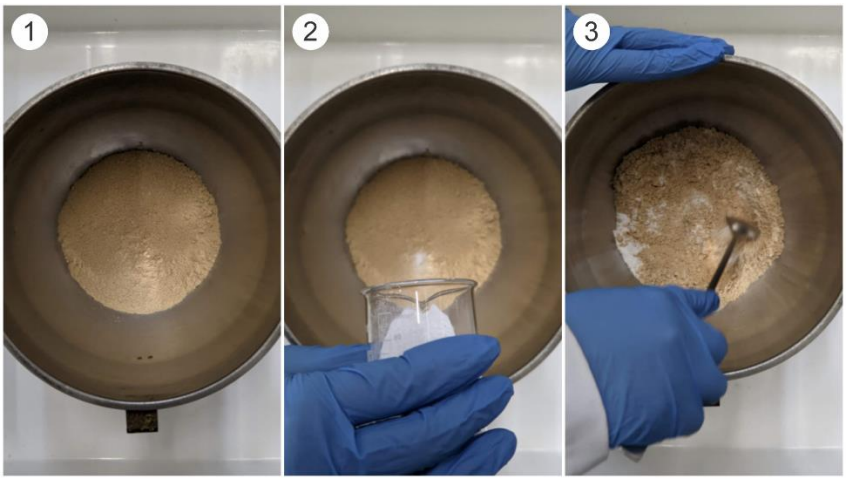

Figure 16: Solid Manual Mixing for Geopolymers Production.

Then, as represented in Figure 17, this solid portion was mixed with the alkaline solution (1) and water (2) in a standardized paddle mixer (3). After that, the fresh geopolymer was placed in a silicone mold and subsequently cured for 4 days at 40 °C and then at room temperature, obtaining a final geopolymer (4).

Figure 17: Final Process of Geopolymers Production.

It is important to note that in the mixing process, three standardized cycles, determined by EN 196-1[19], must be reproduced by the mixer to obtain a fresh geopolymer with good workability. Each of these standardized cycles is divided into two moments; at

the beginning, the rotation of the mixer is 62 rpm for one minute and then 125 rpm for one more minute. Figure 18 shows the evolution of the mixing according to each cycle. The third image represents the final mixture, which has an aspect similar to a non-Newtonian fluid.

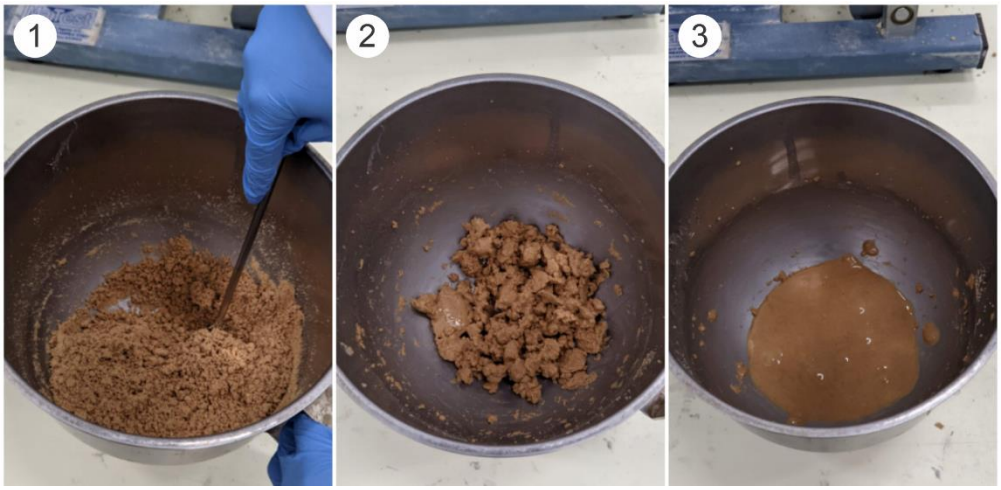

Figure 18: Mixing evolution according to the cycles.

4.2.3.2. Determination of Geopolymers Characterization

The geopolymers produced were characterized by XRD, FTIR, SEM/EDS, and Surface and Pore Analyzer to analyze the material's microstructure. The analyses were performed as described in section 4.2.2.

4.2.4. Determination of Geopolymeric Mortars Synthesis and Characterization

4.2.4.1. Geopolymeric Mortars Synthesis

The geopolymeric mortars were produced in different steps. Figure 19 shows step by step, and Figure 20 shows the practical production.

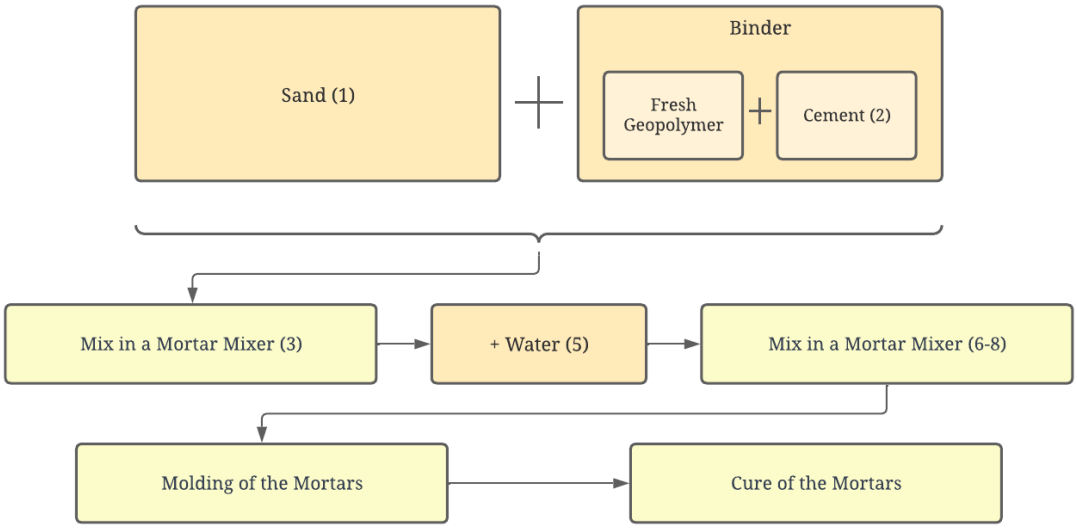

Figure 19: Flowchart of Geopolymeric Mortars Production.

First of all, the fresh geopolymer was obtained as described in 4.2.3.1. After that, it was added sand (1) and cement (2) and mixed for one standardized cycle (3), similarly to the one mentioned in the previous section, obtaining a dry mixing (4). Later, more water (5) was added, and the material was mixed until a workable mortar was obtained (6-8). For this, it was necessary to have three standardized cycles in the end.

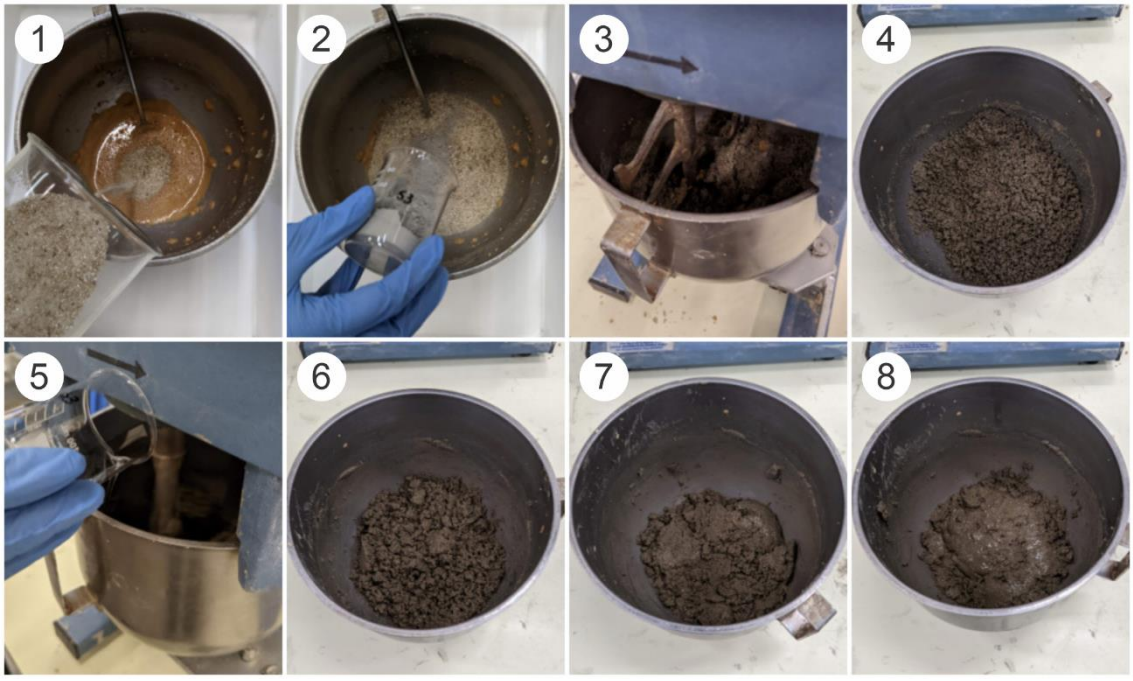

Figure 20: Process of Geopolymeric Mortars Production.

To produce the geopolymeric mortars, the proportion of binder:sand:water was 1:3:X, where X was a range between 0,6 and 0,68 to obtain good workability, evaluated

through a flow test made with the fresh mortar right after the mixing process. It's important to note that the water in the geopolymer composition was considered in the calculation.

After that, the fresh geopolymeric mortar was placed in different molds according to further analysis. For compression and flexural test, acrylic molds (Figure 21) of 40×40×160 mm and 40×40×40 mm were used, respectively.

Figure 21: Geopolymeric Mortars in Acrylic Molds.

Finally, the curing process consisted of letting the samples in an oven at 40 ºC for 4 days, then de-mold them and putting them at room temperature (25 ºC) until they were completed 28 days from the day they were produced.

4.2.4.2. Determination of Geopolymeric Mortars Characterization

The geopolymeric mortars produced were characterized by compressive and flexural tests after 28 days of production, and flow tests. Compressive and flexural tests were made in mortar samples for the compressive and flexural strength analysis of diatomaceous earth geopolymer-based mortars following the European Standard EN 1015-11[100]. The results were given in N/mm^2 (MPa), and the samples were compared. These tests were conducted in triplicate in a Shimadzu - AGS-X-10kN at the Laboratory of Structures and Strength of Materials in the Polytechnic Institute of Bragança (Figure 22).

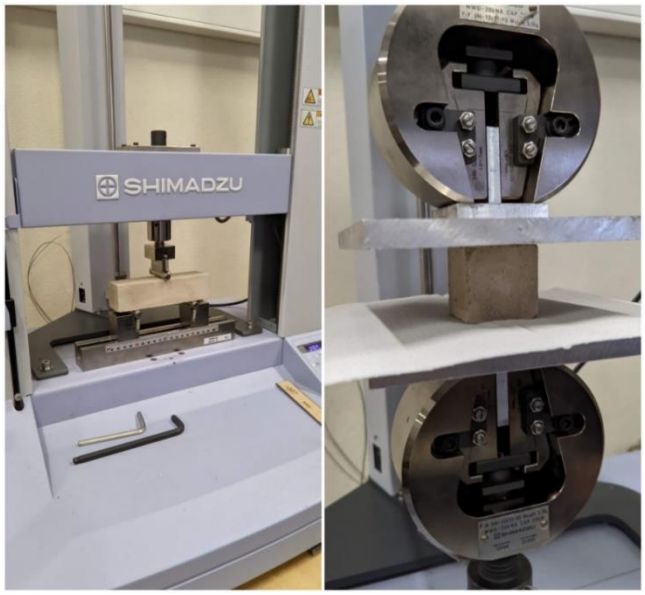

Figure 22: Flexural and Compressive Strength Tests.

To evaluate the workability of fresh mortars (before solidification), it's necessary to analyze their capacity to flow, and it gives a measure of the deformability of the fresh mortars when subjected to a particular type of stress[101].

This analysis aimed to compare the flow between all the geopolymeric mortar samples. The flow test was made in a flow table and followed what is defined in the ASTM (American Society for Testing and Materials) Standard C 1437[102]. The caliper used on this standard is graduated to indicate one-fourth of the actual flow percentage so that the readings of four measurements on the caliper may be added to give the flow value without calculating the average of four individual measurements of the total flow[102]. So, the results are given in percentages of flowing, which makes it possible to compare the samples between themselves.

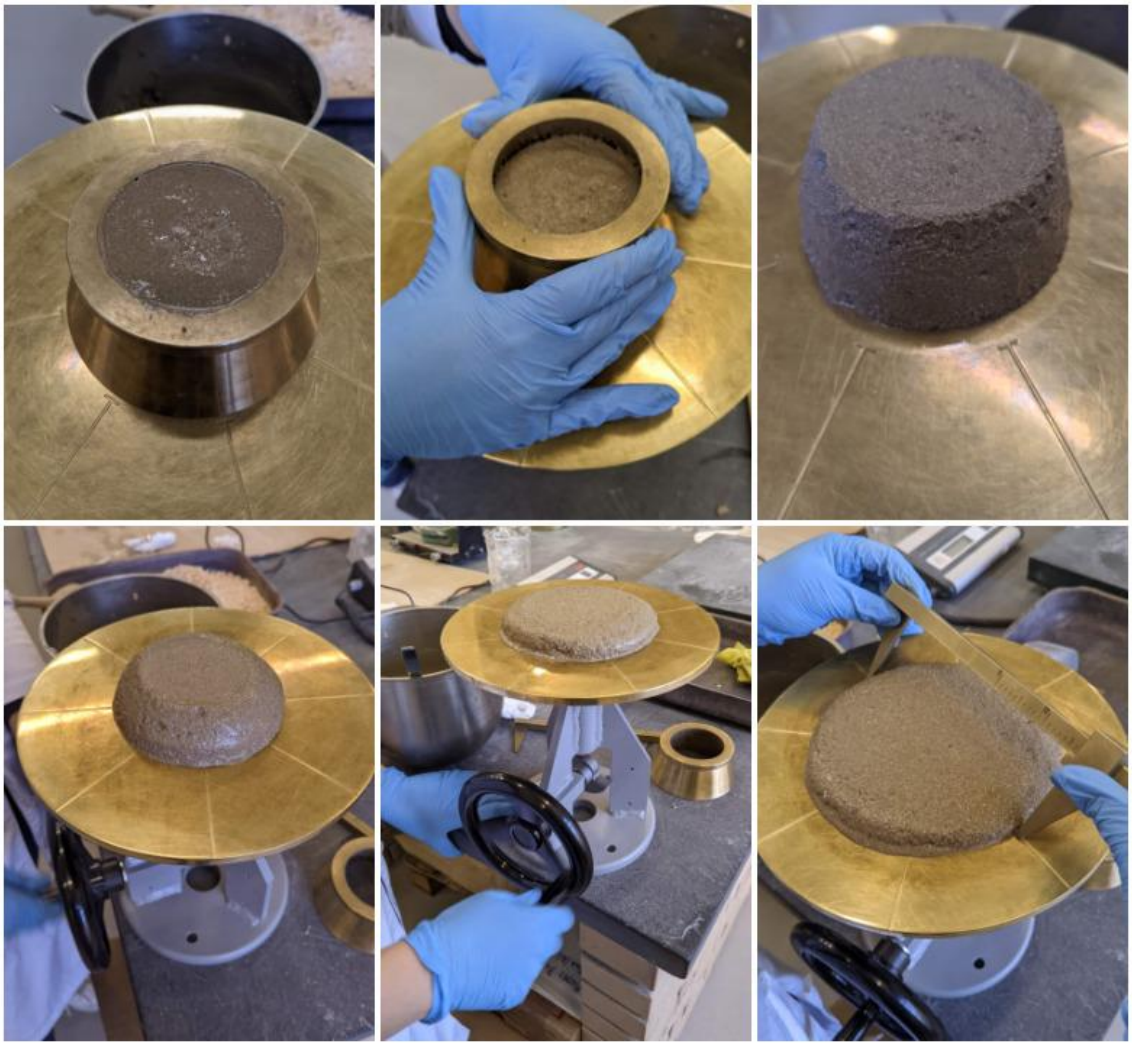

Figure 23: Flow Test.

5. RESULTS AND DISCUSSION

The results of the present work are presented in three parts: the first describes the characterization of the SDE used as a precursor material, the second describes the characterization of the geopolymers produced, and finally, the last part deals with the geopolymeric mortars characterization.

5.1. SPENT DIATOMACEOUS EARTH CHARACTERIZATION

5.1.1. Inductively Coupled Plasma-Optical Emission Spectrometry (ICP-OES)

The data regarding the chemical composition of SDE, obtained by inductively coupled plasma-optical emission spectrometry (ICP-OES), are presented in Table 8. It can be observed that the main elements present are silicon and aluminum, representing 42,10% and 7,44%, respectively, which corresponds to a molar ratio of Si/Al of 6,08. These values approximate the values found in the literature on diatomaceous earth. Vennapusa J et al.[103] discovered an elemental composition of 36,36% of Si, 5,72% of Al an 42,49% of oxygen, indicating that these elements were likely oxidized, as expected for an aluminosilicate material. Baturin G[104] also reported a higher silicon concentration in its oxide, with 44,3% of silica and 3,0% of alumina.

Table 8: Chemical composition of Spent Diatomaceous Earth (wt.%).

Si	Al	K	Fe	Ca	Mg	Mn
42,10	7,44	3,55	0,57	0,56	0,12	0,03

5.1.2. X-Ray Diffraction (XRD)

Figure 24 presents the X-ray diffractogram of SDE. The diffractogram shows the presence of a broad diffuse halo centered at approximately $2\theta = 20\text{-}30°$, indicating the amorphous structure of the precursor material[105]. This confirms previous literature findings that diatomaceous earth is almost pure amorphous silicon dioxide[66]. The amorphous structure is crucial for the geopolymerization reaction, as a more amorphous precursor structure leads to a more extensive reaction as it is widely accepted that the reactivity of aluminosilicate materials is directly proportional to the degree of structural disorder, which is characterized by a higher level of amorphization[106].

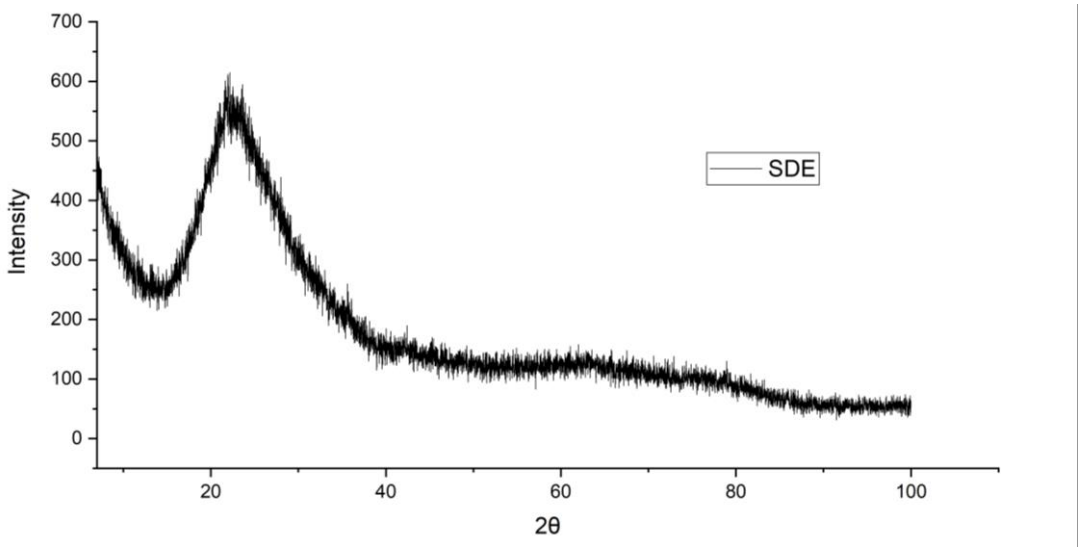

Figure 24: XRD of Spent Diatomaceous Earth.

5.1.3. Fourier Transform Infrared Spectroscopy (FTIR)

The SDE spectrum obtained by FTIR is presented in Figure 25. As illustrated, the peaks detected at 785 and 1020 cm^{-1} have been attributed to DE particles[107,108], which are distinctive features of silica, confirming the previous XRD[109]. The wide band positioned at 1020 cm^{-1} is likely a result of the asymmetric stretching of the Si-O-T bond (T = Si or Al), and the one positioned at 785 cm-1 may be connected to the stretching vibration of the Al-O-Si bonds[110,111]. Although it could also be ascribed to the deformation of O-H bonds or the presence of free silica and the symmetrical stretching of SiO-H bonds, as reported in previous studies[112–114].

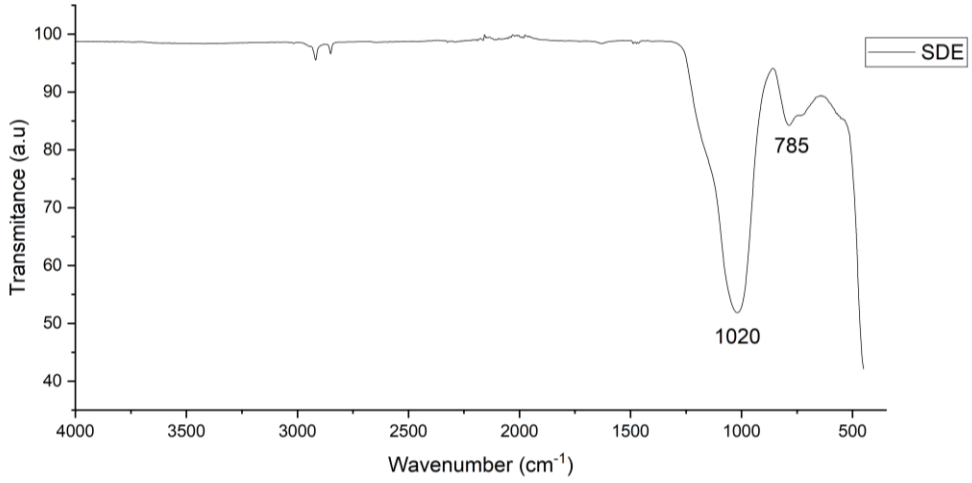

Figure 25: FTIR of Spent Diatomaceous Earth.

5.1.4. Scanning Electron Microscopy with Energy Dispersive X-ray Spectroscopy (SEM-EDS)

As described in section 2.2.1.2 of this thesis, diatomaceous earth is produced by the fossilization of algae known as diatoms, which possess frustules derived from their external skeleton rich in silicon dioxide[66–68]. The literature commonly includes Scanning Electron Microscopy images of diatomaceous earth, which typically display these distinctive frustules for their capsule-like shape and central circular opening[75,115], as Figure 26 depicts.

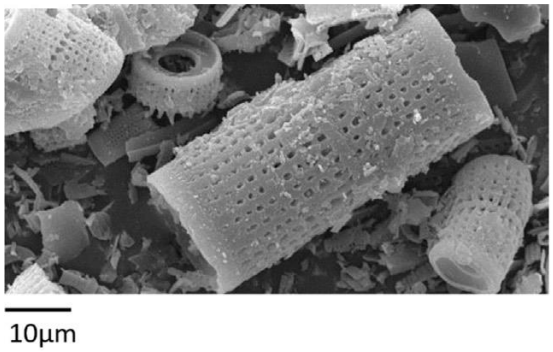

Figure 26: SEM Image of Diatomaceous Earth in the Literature[75].

However, the current study employed an SDE previously utilized as a filter in the wine industry and subsequently underwent a calcination process to eliminate the organic matter. Figure 27 illustrates SEM images of the SDE utilized in producing geopolymers. The images showcase scales of 100, 50, and 20 µm. Observations from the SEM images of the SDE showed no particular shape or crystalline structure, and it instead appeared like flakes.

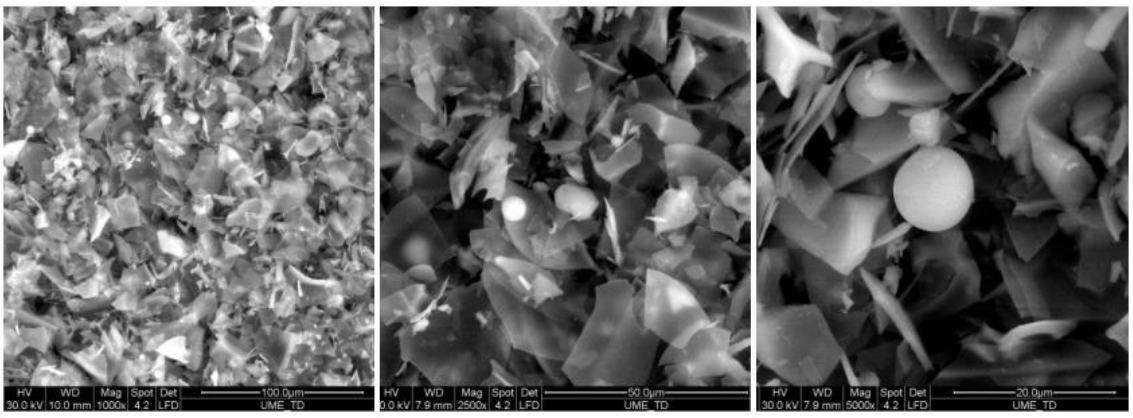

Figure 27: SEM Images of Spent Diatomaceous Earth (scales of 100, 50, and 20µm).

The elemental analysis of the SDE by energy dispersion X-ray, as depicted in Figure 28, confirmed the presence of silicon and aluminum, consistent with the results

obtained from ICP-OES analysis. Furthermore, the EDS analysis revealed that these elements were oxidized, indicating that the SDE is an aluminosilicate material and is suitable for the formulation of geopolymers.

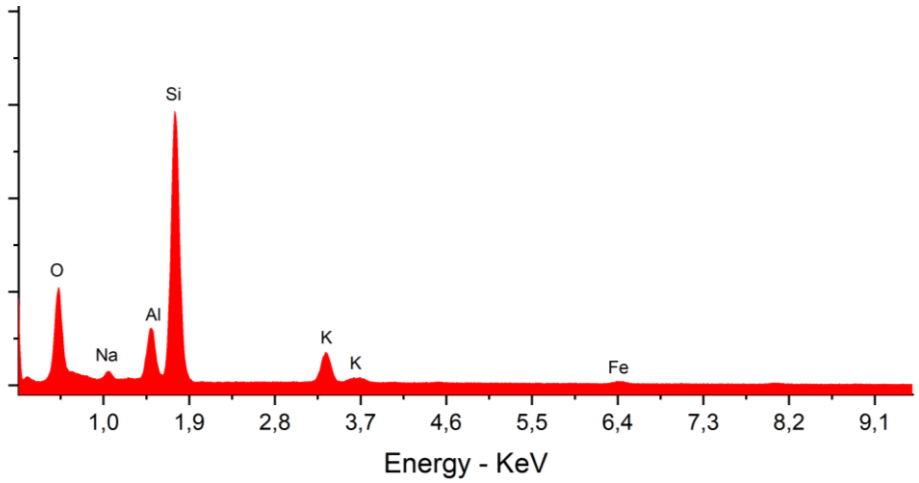

Figure 28: EDS of Spent Diatomaceous Earth.

5.1.5. Surface and Pore Analysis

The structure and properties of geopolymers depend on various raw material characteristics, such as particle size, as mentioned in section 2.2.1.1. This is because the particle size can significantly impact the material's reactivity and, consequently, affect the geopolymerization reaction[116]. Kirschner and Harmuth[117] suggest that the ideal area for raw materials used in geopolymers is between 16 and 29 m^2/g. The pore properties of SDE of this present study have been presented in Table 9 and indicate that its specific surface area meets this ideal range, indicating that it may serve as a suitable precursor material.

Table 9: Pore Structure Parameters of SDE.

Sample	Specific surface area BET (m^2/g)	Pore Volume (cm^3/g)	Average pore radius (nm)
SDE	15,6941	0,0156	1,815

The N_2 adsorption-desorption isotherm and pore size distribution of SDE are illustrated in Figure 29 and Figure 30. It should be noted, according to the physisorption isotherm classification suggested by IUPAC[99], that SDE seems to exhibit a type III isotherm (as shown in Figure 29), which is typical of materials with low porosity[118].

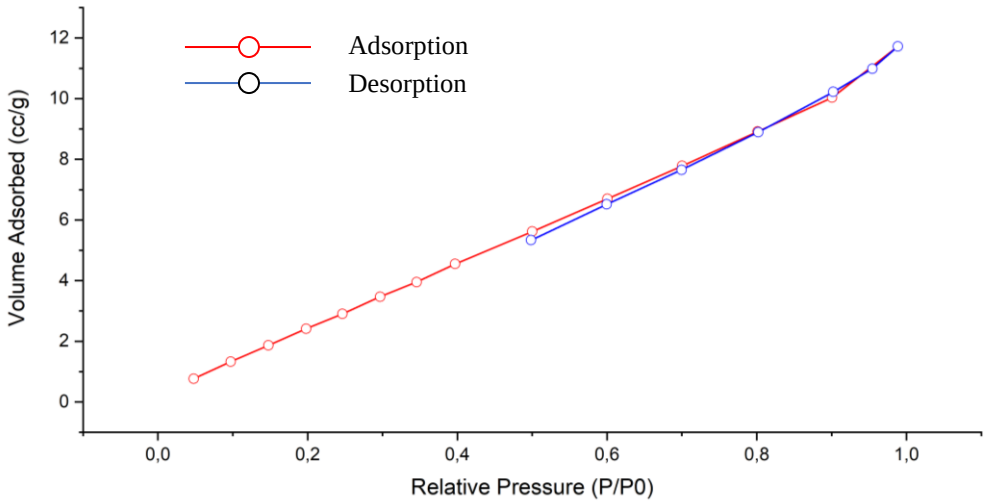

Figure 29: N2 Adsorption-Desorption Isotherm of SDE.

Figure 30 and Table 9 show that most of the pore radius are concentrated around 1,815 nm, indicating that these few pores are mesopores, defined by having major pore diameter distributions between 2-50 nm[99].

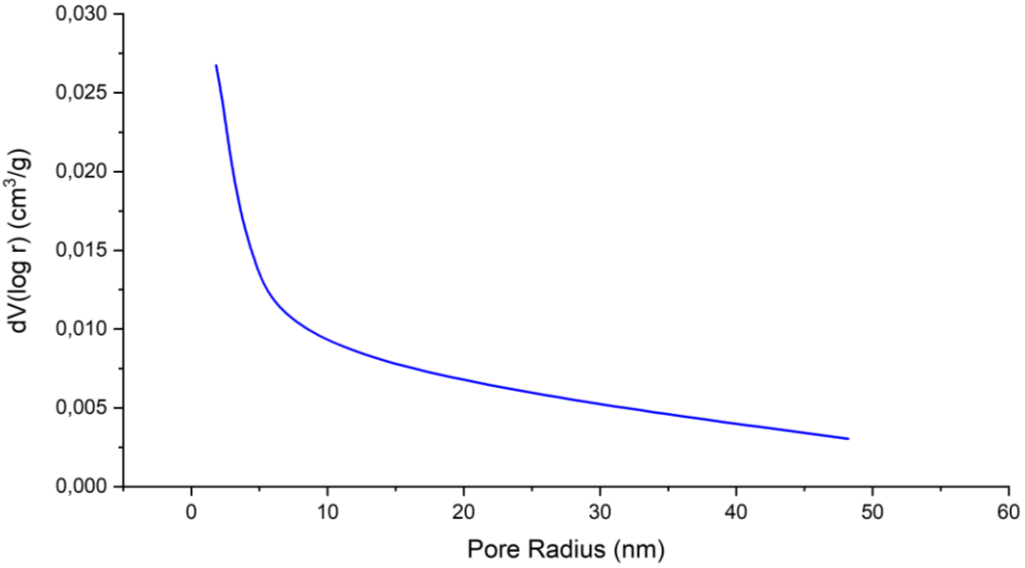

Figure 30: Pore Radius Distribution of SDE.

5.2. GEOPOLYMERS AND GEOPOLYMERIC MORTARS CHARACTERIZATION

5.2.1. Geopolymers Formulation

To determine all formulations of GPs (Table 10), the previously presented ICP-OES of SDE analysis was fundamental, once the exact amount of 42,10% of Si and 7,44% of Al of the precursor was discovered. According to Davidovits [20] and PAPA et al.[118], aluminosilicates' three-dimensional structure and properties, such as mechanical properties, are determined by the silicon/aluminum molar ratio. Rowles and O' Connor[32]

achieved excellent compressive strength with a 2,5 ratio, while He P et al. [119] attained excellent mechanical properties with 3,5. Then, Si/Al ratios of 2,5 and 3,5 were chosen for this study. However, our precursor had a ratio of 6,08, so it required the addition of alumina to increase the proportion of aluminum and bring the Si/Al ratio to an appropriate level.

As previously mentioned in section 4.2., two distinct concentrations of NaOH were selected for comparison based on their impact on the structure and properties of the resulting geopolymer, once it is essential to have enough OH^- and Na^+ íons to dissolve the aluminum present in the precursor material and to balance the negative charge of the $Al(OH)^{-}$[120], allowing the geopolymer structure to be formed, as described in section 2.2. Regarding mechanical properties, Ibrahim W et al.[121] achieved higher compressive strength using a 12M NaOH solution, whereas Yahya Z et al.[122] obtained better compressive results with a 10M concentration. So, following this literature and what was presented in section 2., the concentrations utilized in the present study were 10M and 12M.

Thus, GP1 and GP2 were prepared using a NaOH solution of 10M, while GP3 and GP4 were prepared using a solution of 12M. Regarding the Si/Al ratio, GP1 and GP3 had a ratio of 2,5, while GP2 and GP4 had a ratio of 3,5. The mass ratio of NaOH to SS was 0,5, and the quantity of SS was determined by a mass ratio of SS/precursor of 0,4, where the precursor was SDE and alumina. The amount of water was selected to attain a homogeneous geopolymer paste during the mixing process. Using less water than utilized prevented the mixture from forming a paste.

Table 10: Geopolymer's Formulation.

Sample	sDE (g)	Al_2O_3 (g)	NaOH (M)	NaOH (g)	SS (g)	Water (g)
GP1	23,7	8,87	10M	6,51	13,03	35,82
GP2		4,80		5,70	11,40	
GP3		8,87	12M	6,51	13,03	
GP4		4,80		5,70	11,40	

Following the curing process outlined in item 4.2.3.1., the resulting geopolymer is depicted in Figure 31. All four geopolymers exhibit the same visual characteristics.

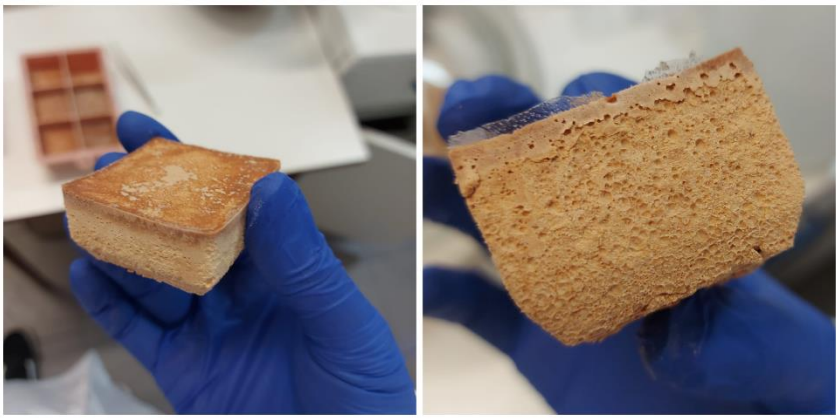

Figure 31: Spent Diatomaceous Earth-based Geopolymer Produced.

5.2.2. Geopolmeric Mortars Formulation

Table 11 illustrates the formulation of geopolymeric mortars based on the proportions outlined in item 4, the results of the SPD ICP-OES analysis and the geopolymer formulation. Samples S1 to S4 employed a 75% geopolymer and 25% cement binder, whereas S5 to S8 utilized a binder of 90% geopolymer and 10% cement. Samples S9 to S12, on the other hand, relied solely on a binder of 100% geopolymer.

Table 11: Geopolymeric Mortars Formulation.

		Geopolymeric Binder						Mortar		
Sample	**GP in the Binder (wt%)**	**SPD (g)**	**Alumina (g)**	**NaOH (M)**	**NaOH (g)**	**SS (g)**	**GP Water (g)**	**Cement (g)**	**Sand (g)**	**Mortar Water (g)**
S1	75%	17,78	6,65	10	4,89	9,77	26,87	13,03	156,33	4,40
S2			3,60		4,28	8,55	26,87	11,40	136,81	0,49
S3			6,65	12	4,89	9,77	26,87	13,03	156,33	4,40
S4			3,60		4,28	8,55	26,87	11,40	136,81	0,49
S5	90%	21,33	7,98	10	5,86	11,72	32,24	5,21	156,33	1,63
S6			4,32		5,13	10,26	29,64	4,56	136,81	-
S7			7,98	12	5,86	11,72	32,24	5,21	156,33	1,63
S8			4,32		5,13	10,26	29,64	4,56	136,81	-
S9	100%	23,70	8,87	10	6,51	13,03	35,43	-	156,33	-
S10			4,80		5,70	11,40	31,01	-	136,81	-
S11			8,87	12	6,51	13,03	35,43	-	156,33	-
S12			4,80		5,70	11,40	31,01	-	136,81	-

The mortars' geopolymeric binders are the exact composition of GP1, GP2, GP3 and GP4, varying according to the amount of cement. So, for example, S1, S5, and S9 have the same composition as the GP1 on their geopolymeric binder, and S2, S6, and S10 have the exact composition of GP2; this logic was followed for the others.

Following the curing process outlined in item 4.2.4.1., the resulting geopolymeric mortar is depicted in Figure 32.

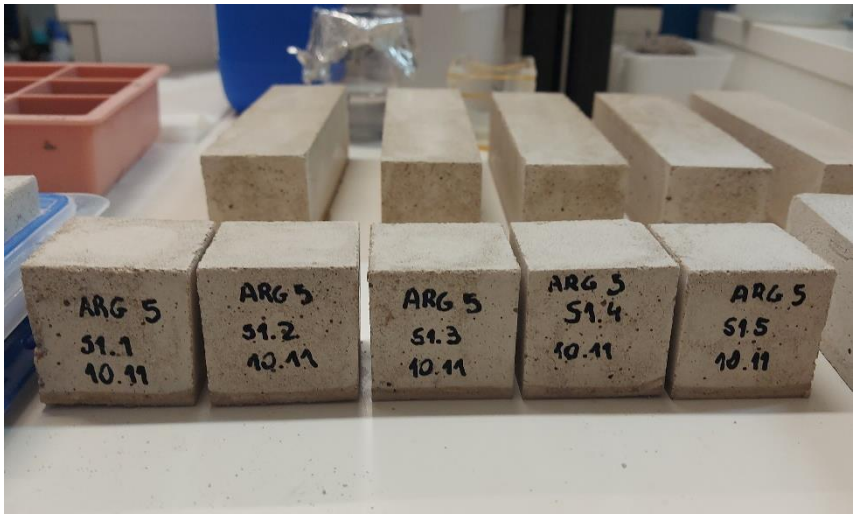

Figure 32: Geopolymeric Mortars Produced.

5.2.3. Geopolymers Characterization

5.2.3.1. X-Ray Diffraction

Figure 33 shows the diffractogram of diatomaceous earth and geopolymers with different NaOH concentrations and Si/Al ratios, as described in item 5.2.1.

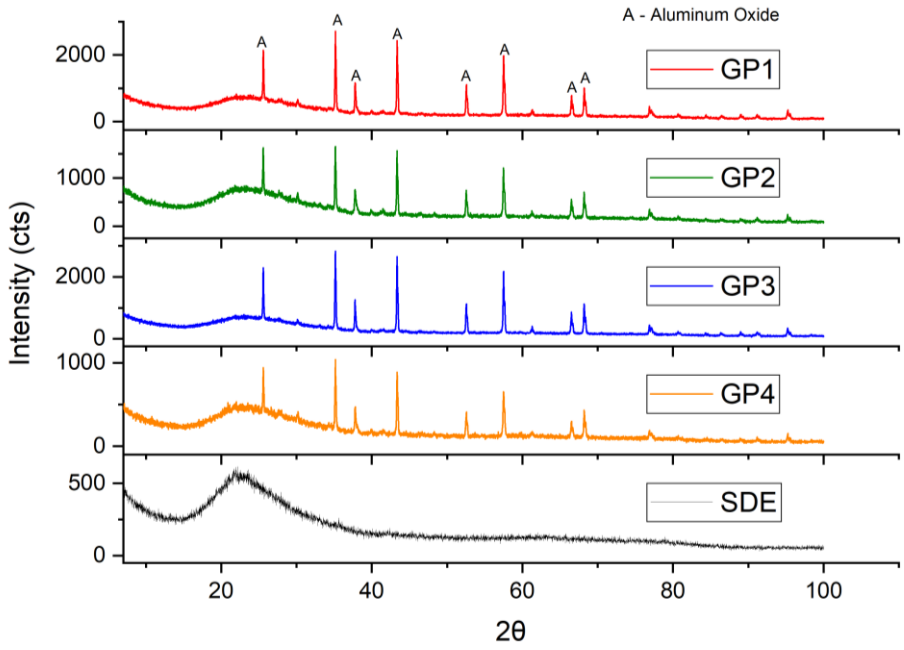

Figure 33: XRD results for GPs.

The appearance of crystalline peaks is observed in the XRD analysis of geopolymers compared to that of diatomaceous earth. The major ones are associated with the aluminum oxide phase at 25.57º, 35.14º, 37.77º, 43.35º, 52.54º, 57.48º, 66.51, and 68.20º in all four GPs[123,124]. These peaks originate from the alumina added to the precursor, some of which are repeated in the diffractogram of the geopolymers. The alumina pattern is shown in Figure 34, and it can be seen that the resulting geopolymers do not have all the peaks present in the raw material, as the ones at 41.61º, 46.18º, 59.77º, 70.36º, 74.27º, 85.19º and 90.66º, confirming a certain degree of consumption of this alumina in the geopolymerization reaction[125].

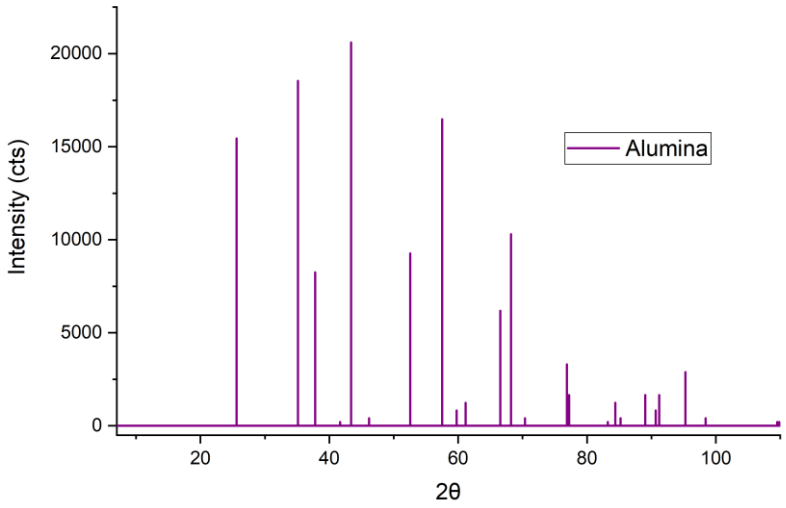

Figure 34: XRD Pattern for Alumina.

However, the prominent peaks persisted, although with significantly reduced intensity, indicating the presence of partially unreacted crystalline material. This suggests that Al_2O_3 didn't completely dissolve in the alkaline solution, which may have an impact on the geopolymerization reaction since the alumina added to compensate for the low level of it in the diatomaceous earth should promote the polymerization process by producing a significant amount of $Al(OH)^4$ when reacting with the alkaline solution[125].

When comparing geopolymers based on their Si/Al ratio, it can be observed that GP1 and GP3 exhibit more pronounced peaks of aluminum oxide compared to GP2 and GP4. This can be attributed to the fact that GP1 and GP3 have Si/Al ratios of 2,5, which indicates a higher amount of alumina present in the geopolymer, in contrast to GP2 and GP4, which have Si/Al ratios of 3,5. The higher alumina concentration in GP1 and GP3 likely contributes to the observed differences in aluminum oxide peaks between these materials and GP2 and GP4.

As described in section 5.1, the presence of a broad and diffuse halo centered at approximately 2θ = 20-30° is observed in the SDE, indicating the presence of an amorphous phase. In the diffractograms of the four GPs in Figure 33, a similar halo is observed at approximately the same position but with varying intensities. When compared with the diffractogram of the SDE, the intensity of the halo in the GPs has increased, which indicates a more considerable amount of the amorphous phase. This, in turn, suggests a greater quantity of the geopolymer phase present in the samples[126], especially in GP2. In the literature, this amorphous phase described by the halo usually indicates the NASH structure (sodium alumino-silicate hydrate) gel formation[120,127], so it's possible to assume the same in this work, and this is reinforced by posterior analysis, like EDS.

In the section 2.2, the geopolymerization process was described by four mechanisms. They are influenced by the amount of alkaline solution and its concentration once the amount of OH^- and Na^+ needs to be sufficient to dissolve the aluminum from the precursor and to balance the negative charge of the $Al(OH)^-$, respectively. If there is more aluminum than the maximum for the reaction, less NASH gel is generated, and more unreacted Al is presented[120]. This is a possible explanation for why the amorphous halos of GP1 and GP3 are less intense than GP2. The first and the third samples have a Si/Al of 2,5, so the amount of aluminum oxide powder added to the precursor was higher,

causing an excess of Al. This also goes according to the conclusion of unreacted aluminum described by the intensity of the crystalline peaks.

It can be a sign of a few crystalline phases of zeolite that XRD couldn't detect due to its small quantity. In GP4, however, it can be noticed that the crystalline peaks and the amorphous halo have lower intensities than the other samples. It's possible to assume this once the chemical composition and structure of NASH gel are similar to the zeolites, and this last one has a greater tendency to be formed in high concentrations, which is the case of GP4 (12M)[127].

5.2.3.2. Fourier Transform Infrared Spectroscopy

Figure 35 presents the results obtained by FTIR of SDE and all the geopolymers. As described in section 5.1, the highest intensity peak corresponding to the adsorption band in 1020 cm^{-1} can be related to the vibration of the asymmetric stretching of the Si-O-Si bond, which can be seen in SDE and GPs samples.

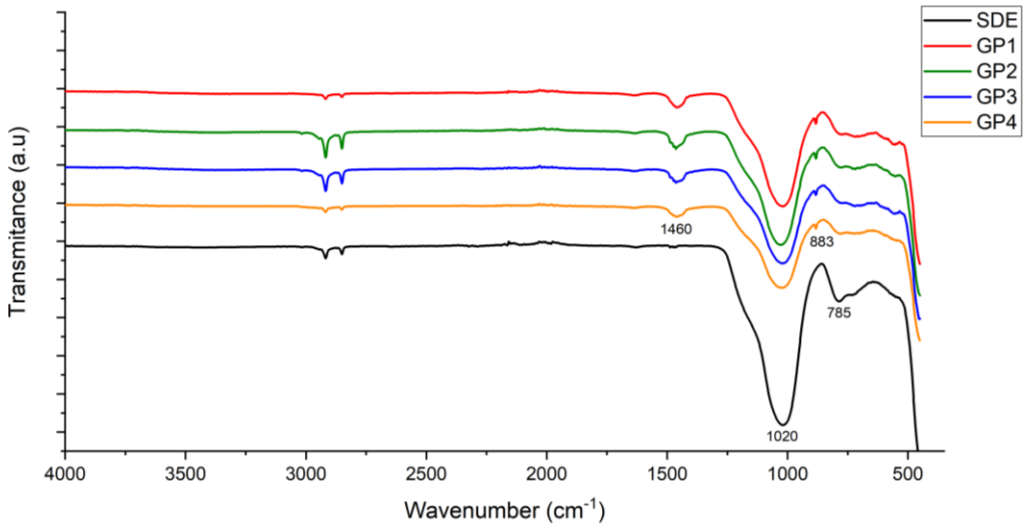

Figure 35: FTIR results for GPs.

Studies in the literature examining the correlation between the Si/Al ratio caused by geopolymerization and the frequency (cm^{-1}) at which peaks occur concluded that an increase in the quantity of Al components results in a gradual shift of the peaks generated through geopolymerization to lower frequencies[128]. However, the results of this present work show that the highest intensity peak observed in GPs did not exhibit any significant dislocation. This observation can be attributed to the findings of the XRD analysis, which revealed that not all of the alumina was involved in the geopolymerization process. As a

result, there was a deficiency in forming a strong Si-O-Al bond, which was expected to occur in frequencies close to 990 cm^{-1}, according to the literature[105].

In the FTIR analysis of geopolymer samples, the emergence of new bands near frequencies of 883 and 1460 cm^{-1} can be observed when compared to the raw material. The band at 1460 cm^{-1} corresponds to the antisymmetric vibrations of CO_2^3 ions, indicating the presence of sodium carbonate in the geopolymer's structure. Additionally, the absorption band at 883 cm^{-1} is associated with the Si-O-Al stretching vibration[129;] following XRD analysis, a specific part of alumina reacted in the geopolymerization process.

5.2.3.3. Scanning Electron Microscopy with Energy Dispersive X-ray Spectroscopy

Figure 36 presents the SEM images of the produced GPs. GP1 and GP3 samples, which have the same Si/Al ratio of 2,5, exhibited the irregular shapes and sizes of a flocculent morphology covered with fine powder spheres[127]. These attached spheres can be due to the higher quantity of alumina powder added to these samples to achieve the desired Si/Al ratio[129], but they didn't react, reinforcing the XRD analysis. These images also exhibited smaller pores e more compact structures.

Meanwhile, GP2 and GP4 samples presented mainly a flocculent morphology with more prominent pores and a less compact structure. Also, needle-like structures were detected in GP4. This type of structure is similar to zeolitic-fibrous phases, which can propose a small amount of a poor crystalline phase of zeolite in the sample[127,130], going according to what was analyzed in XRD.

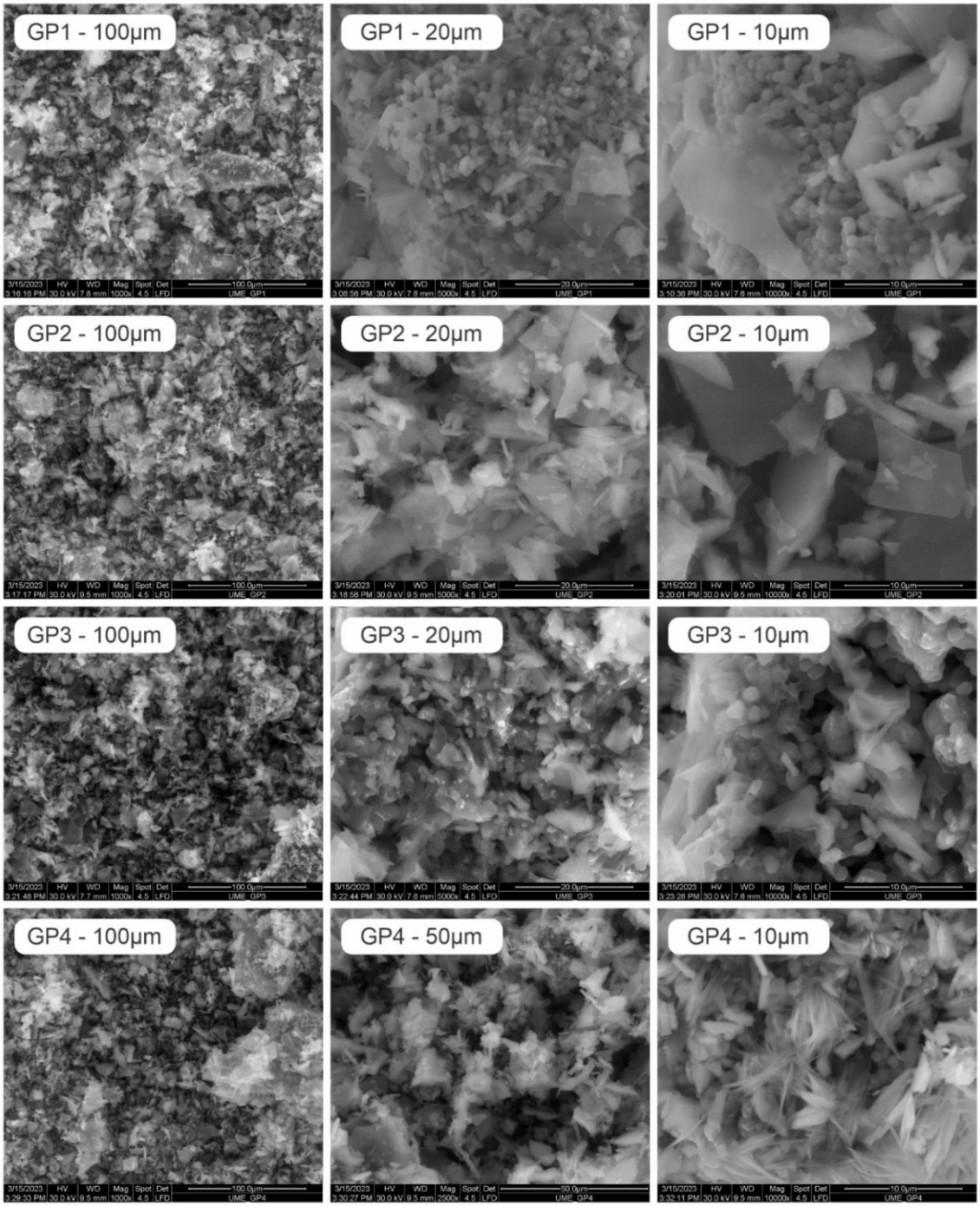

Figure 36: SEM Images of GPs.

The elemental analysis of the geopolymers by energy dispersion X-ray, as depicted in Figure 37, showed the presence of silicon, aluminum, and oxygen, which was consistent with the expected results of a polysialate material[20]. Compared to the SDE's EDS result, it was observed that the intensity of Si, Al, O, and Na had increased. The presence of sodium was intensified by using NaOH solution, which served as the alkaline solution to prepare geopolymers. The silicon and aluminum content increase can be attributed to adding SS solution and alumina powder, respectively. These results align

with the findings of the FTIR analysis, which indicated the formation of a Si-O-Al bond at the absorption band of 883 cm^{-1}.

The graphics also indicate that the intensity of the silicon peak is higher in GP2 and GP4 compared to GP1 and GP3, which confirms the higher Si/Al ratio desired in GP2 and GP4 formulation. Furthermore, this composition helps assume that there was a NASH formation[130], as described in the XRD analysis.

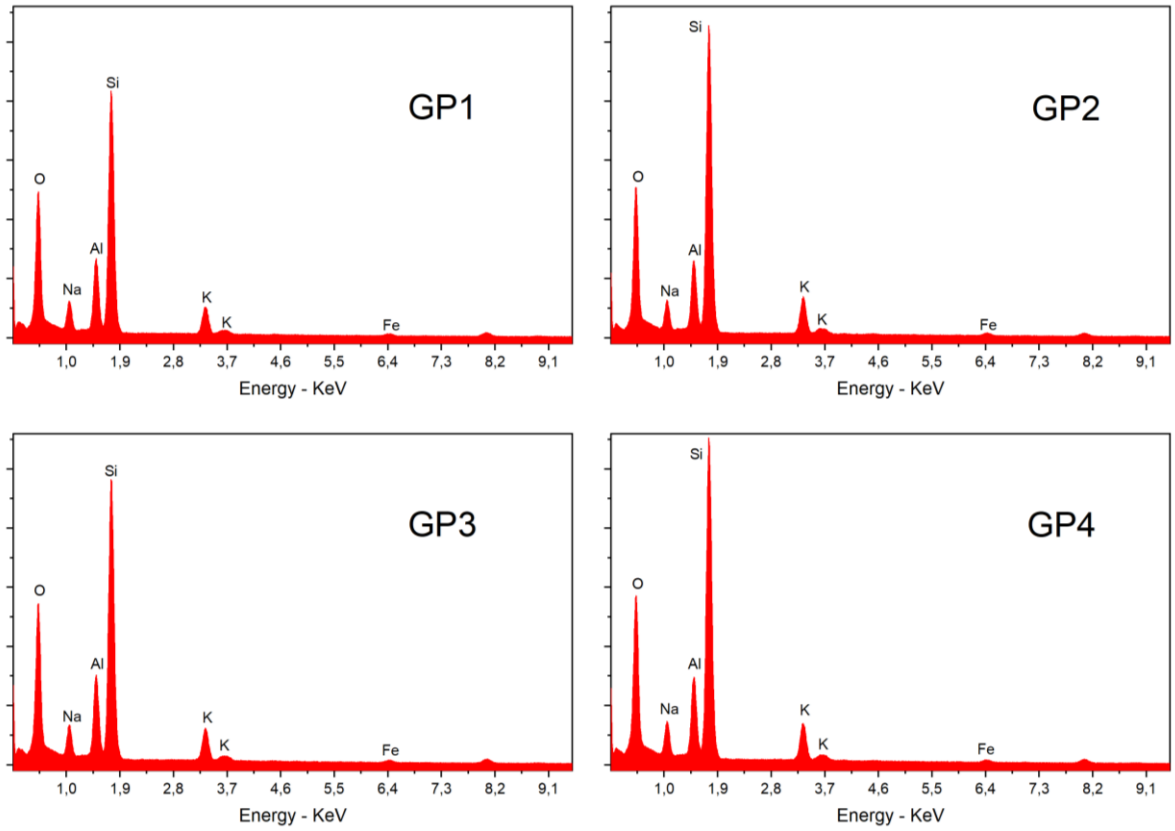

Figure 37: EDS results for GPs.

5.2.3.4. Surface and Pore Analysis

The N_2 adsorption-desorption isotherm and pore size distribution of GPs are illustrated in Figure 38 and Figure 39, respectively. According to the physisorption isotherm classification suggested by IUPAC[99], it should be noted that GP1, GP3, and GP4 seem to exhibit a type III isotherm, typical of materials with low porosity[118], following the same characteristics of the precursor SDE.

Figure 39 shows that most of the pore radius of GP1, GP3, and GP4 are concentrated around 1,818, 1,813, and 1,812 nm, respectively, indicating that these few pores are mesopores[99].

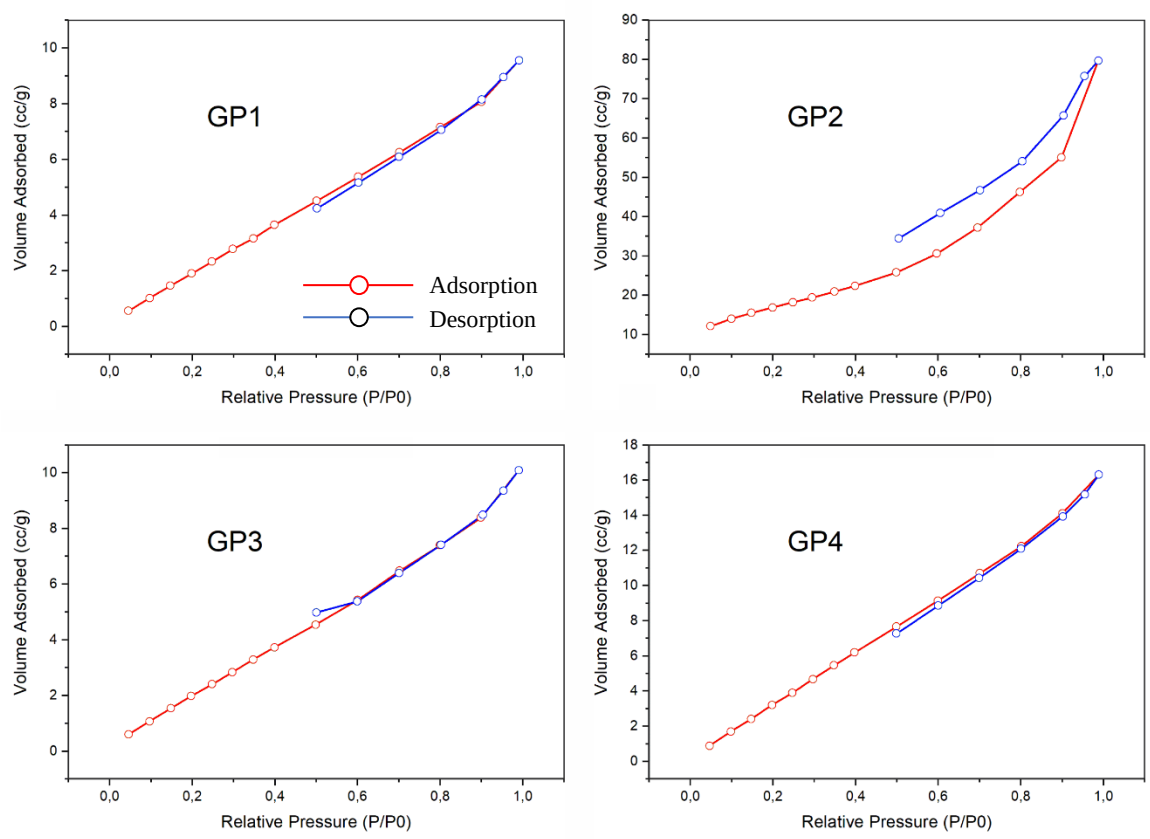

Figure 38: Geopolymers Isotherms.

GP2, as described before, is the sample with more NASH or geopolymeric phase, so this pores analysis follows the literature, which indicates that the more geopolymeric phase, the more the material will have mesoporous characteristics, once this is the most common type of pores in the geopolymer gel[131]. The GP2, however, presents a type IV isotherm, indicating that the sample may be a mesoporous material. This agrees with the pore radius distribution of GP2, reported in Figure 39, which shows an intensive concentration of pores in a radius of 2,305 nm, and with the SEM image, which shows bigger pores compared to the other samples. Figure 38 also shows the difference between the volume adsorbed by GP2 and the other GPs, indicating an elevated specific surface area on the sample, as shown in Table 12 through BET methodology.

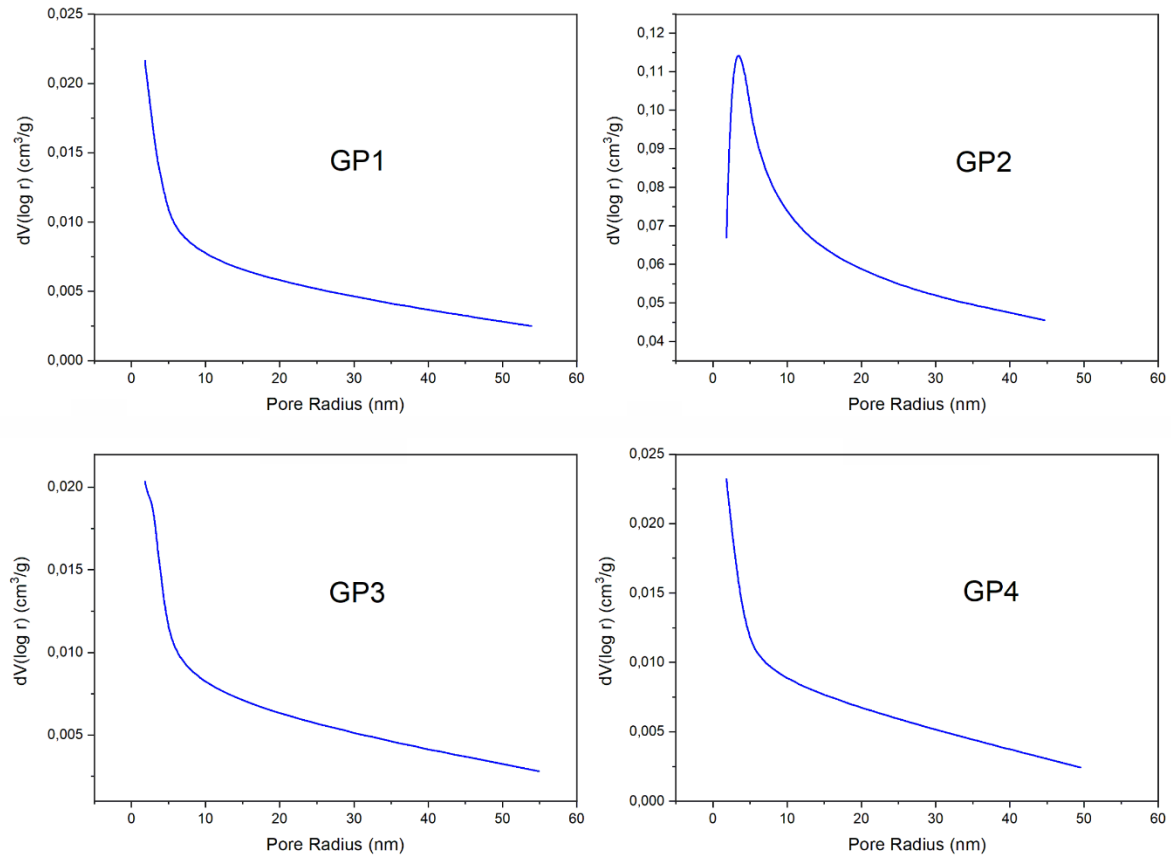

Figure 39: Pore Radius Distribution of GPs.

Table 12 depicts the textural properties of all samples. GP2 and GP4 present a specific surface area more extensive than GP1 and GP3, especially GP2, with an S_{BET} four times bigger than the SDE sample. It brings a positive property to the sample once a higher surface area represents higher reactivity, resulting in higher compressive strength[116]. Also, GP1 and GP3 may have a small S_{BET} due to the particles of the unreacted aluminum shown in SEM images, which can occupy space on the surface, reducing its area and the material's reactivity.

Table 12: Pore Structure Parameters of SDE and GPs.

Sample	Specific surface area BET (m^2/g)	Pore Volume (cm^3/g)	Average pore radius (nm)
SDE	15,6941	0,0156	1,815
GP1	12,8111	0,0127	1,818
GP2	60,9586	0,1104	2,305
GP3	12,9949	0,0135	1,813
GP4	23,2992	0,0219	1,812

5.2.4. Geopolymeric Mortar Characterization

5.2.4.1. Compressive and Flexural Tests Results

As previously mentioned, different samples of geopolymers, namely GP1 to GP4, were examined for their complete or partial application as the binder in mortars. The mortar samples were classified into 12 distinct types. Mortars labeled S1 to S4 contained a blend of 75% geopolymer and 25% Portland cement binders. Specifically, S1 employed the geopolymer GP1, S2 used GP2, S3 used GP3, and S4 utilized GP4. Furthermore, mortars labeled as S5 to S8 were also based on geopolymers, where S5 used GP1 and S8 used GP4, but with a different binder composition consisting of 90% geopolymer and 10% Portland cement. Lastly, S9 to S12 followed a similar pattern, with S9 using GP1 and S12 using GP4 but with a binder consisting of 100% geopolymer.

So, knowing the logic of each sample, it's necessary to analyze the influence of the properties described in section 5.2.3 and on the mechanical behavior of the samples produced with the geopolymers studied previously. Firstly, Figure 40 and Figure 41 show the average values of compressive and flexural strength, respectively (details in appendix). These tests were made in triplicate after 28 days of mortars production.

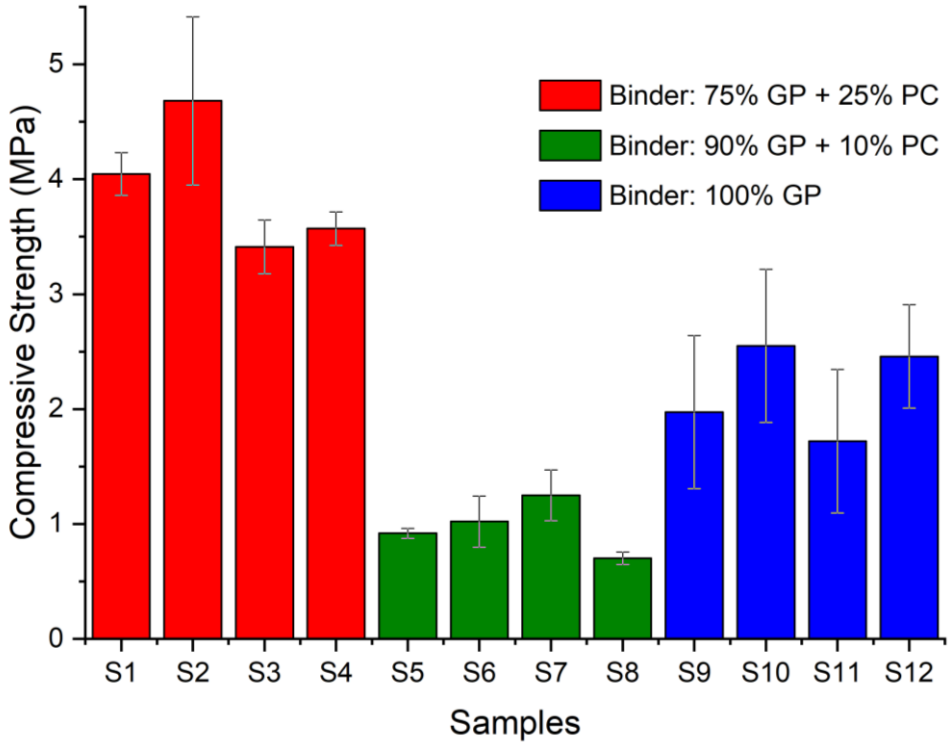

Figure 40: Compressive Strength of Geopolymeric Mortars.

The content of the binder has a significant influence on the material's properties. The primary observation is the difference between the groups S1-4 to S5-8 to S9-12. The group S1-4, having an amount of 25% of Portland cement on the binder, enabled a reaction between the calcium content of PC with the NASH gel of GPs, giving evidence that calcium substituted NASH gels ((C,N)-A-S-H) and calcium aluminate silicate hydrate (CASH) was formed.

Cementitious mortars usually form products as CSH or CASH (calcium aluminate silicate hydrate), producing a stable, amorphous solid hydrate, as described in section 2.1, while geopolymeric mortars usually form products as NASH, as it was studied in section 5.2.3. Not-hybrid mortars, i.e., those that don't mix cement with geopolymer, produce their characteristic product. This happens because PC has a high calcium content, and geopolymers are a low Ca content material[132].

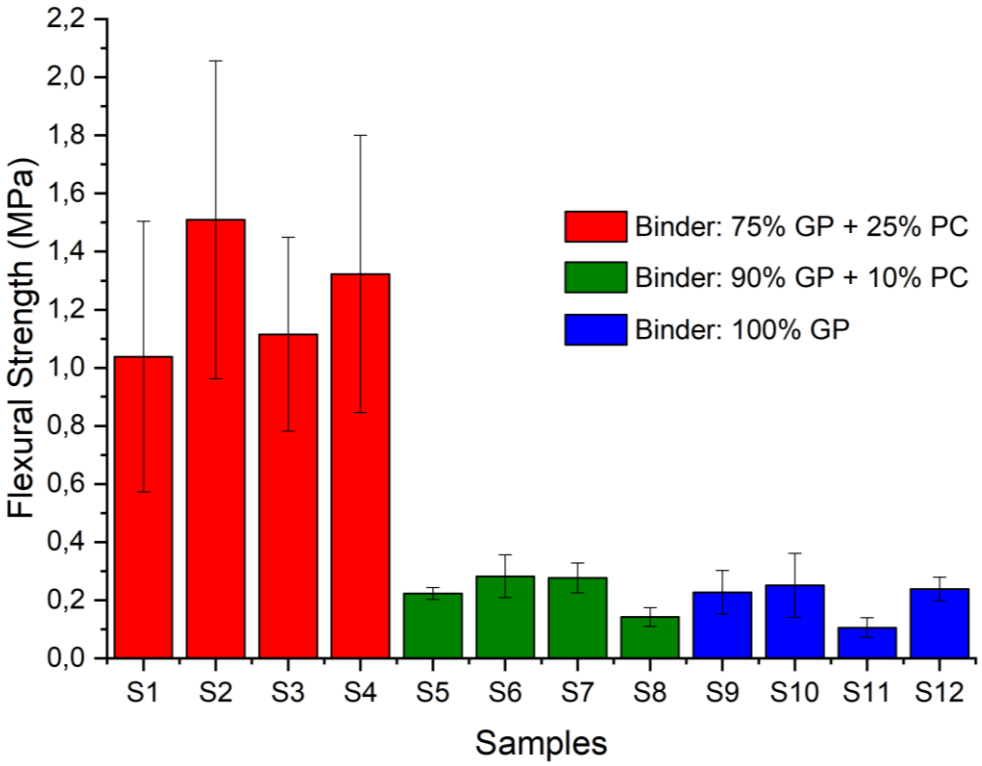

Figure 41: Flexural Strength of Geopolymeric Mortars.

However, some studies showed possible compatibility between CASH and NASH, forming (C,N)-A-S-H gel (calcium substituted NASH gels), where sodium partially is replaced with calcium in hybrid Portland cement–geopolymer systems. In a stable structure with sufficient calcium to produce this, the new product can lead to a higher mechanical strength[132].

In the case of this thesis, there is evidence of this mechanism described once the samples with 25% of cement on the binder (S1 to S4) presented higher compressive (between 3,41 and 4,68 MPa) and flexural strength (between 1,04 and 1,51 MPa). However, the samples with only 10% of PC on the binder (S5 to S8) showed shallow properties, while the utterly geopolymeric mortar samples (S9 to S12) had intermediate values, even without any high calcium content. The stability of the products can explain it. While NASH gels induce a stable system, which can provide good properties, the low-Ca content of the samples S5-S8 may have led to an unstable (C, N)-A-S-H gel[132] formation.

Now comparing the samples between themselves, i.e., in the same group of binder content, it's notable that GP2 binder provides higher mechanical strength. This can be explained by the higher amount of amorphous geopolymer phase described in section 5.2.3. This observation follows some studies which concluded that the compressive strength of geopolymers increased as the crystalline content decreased[133].

Furthermore, the higher reactivity of GP2 and GP4 is due to their high specific surface area studied in 5.2.3. enables a higher interaction with the other components of the mortar, creating a more cohesive structure. This is also confirmed by the higher compressive and flexural strength of almost all the mortar samples composed of geopolymeric binder GP2 (S2, S6, and S10) and GP4 (S4 and S12) when compared to the other samples in the same group.

5.2.4.2. Flow Test Results

Figure 42 presents the flow test made in the fresh geopolymeric mortars (details in appendix). It's clear that S1 to S4 presented a lower flowing than the others. These sample binders comprise 25% of Portland cement, which can be the reason for these results. As described in section 2.1., PC needs water to produce a solid phase that continues to grow and expand in the presence of water and cohesively encapsulates other materials inside the matrix of hydrate solid[17]. So, in this way, the water reacted with the PC, not providing so much fluidity for it compared to those with less or no cement in the composition. Nevertheless, all samples showed good flowability, capable of being used.

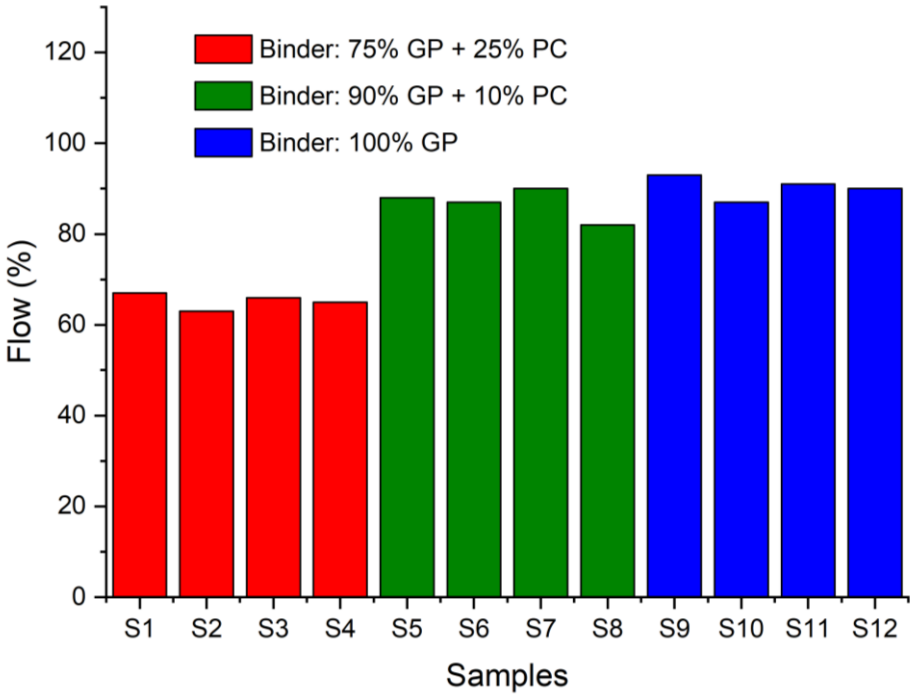

Figure 42: Flow Test Results of Geopolymeric Mortars.

5.2.4.3. Final Discussion

In the literature, it's challenging to find good sources of the use of diatomaceous earth as the precursor of the geopolymer binder, but with different precursors, many kinds of research found excellent mechanical strengths without cement. For example, Sathonsaowaphak[134] used bottom ash as a precursor and achieved around 40-50 MPa in a compressive strength test using 10M and 12M as NaOH concentrations. Islam et al.[135] made a geopolymer mortar comprising different percentages of GBFS, POFA, and FA. GBFS contain large amounts of CaO, while POFA and FA are more similar to SDE, with higher silica concentration. He found a compressive strength of 66 MPa when mixed with 70% of GBFS and 30% of POFA on the precursor and inferior strengths of 18 and 9 MPa, when the precursor was composed of 100% of POFA and 100% of FA, respectively, showing the influence of CaO on the mechanical properties.

Rowles and O' Connor[32] reported a maximum strength of 64 MPa using a Si/Al ratio of 2,5:1 in synthesizing a metakaolin-based geopolymer, and Zhang P.[79,89] produced a metakaolin/fly-ash-based geopolymer, and through compressive strength, test showed a compressive resistance of around 45 MPa.

Compared to the current thesis, the higher strengths observed in the precursors mentioned above can be attributed to the difference between their composition and the

SDE. Analyzing Table 13, where these compositions are displayed, it is evident that most of these precursors have a significant Al_2O_3 content, thereby eliminating the necessity of adding alumina powder to offset it, as with the SDE.

Table 13: Precursors Composition in the Literature.

Author	Precursor	% of SiO_2	% of Al_2O_3	%CaO
Islam et al.[135]	GGBS	32,52	13,71	45,83
	POFA	63,41	5,55	4,34
	FA	54,72	27,28	5,31
Sathonsaowaphak[134]	Bottom Ash	39,3	21,3	16,5
Rowles and O' Connor[32]	MK	53,32	41,85	0,13
Zhang P.[79,89]	MK	54,0	43,0	< 0,8*
	FA	52,0	18,0	12,4*

* Amount of CaO + MgO (%)

So, typically, researchers employ aluminosilicate materials with substantial quantities of alumina and silica within the same raw material. Occasionally, additional materials are introduced to enhance the concentrations of these components. However, the SDE material does not have sufficient alumina, as confirmed by the analysis using ICP-OES. To compensate, alumina powder was added, but it seems that it was not effective, as unreacted alumina particles were found in the XRD and SEM images. This difference might explain why the results of the present thesis diverge from the findings mentioned in the existing literature.

Still, SDE has proven to be an excellent silica source for developing geopolymeric mortars, especially due to its sustainability. Extensive research in Section 2.1. and the existing literature confirms that producing one ton of cement necessitates approximately 2.8 tons of raw materials[136,137]. This conventional process depletes valuable resources like limestone and shale for manufacturing cement clinkers, leading to resource exhaustion. In contrast, SDE is a solid waste generated by the wine industry and can also be obtained

from the beer industry. So, its use as a precursor in geopolymeric mortars minimizes the use of non-renewable resources and waste production[51,52].

The production of Portland cement requires a substantial energy input, releasing a significant amount of carbon dioxide into the atmosphere. On average, the production of one ton of cement in a typical cement factory consumes approximately 110-120 kWh, primarily during the calcination process, which involves temperatures as high as 1500 ºC[138,139]. Furthermore, traditional mortar is typically made using a cementitious Portland cement binder. Meanwhile, as a precursor for geopolymers, SDE only requires a pre-treatment temperature of 700 ºC, making it a more energy-efficient alternative.

Lastly, as discussed in section 2.1, it is essential to address the issue of CO_2 emissions into the atmosphere. The primary source of these emissions is the decomposition of calcium carbonate into calcium oxide during cement production[13]. In contrast, SDE requires treatment at 700 ºC to eliminate volatile compounds, oxidize organic matter, and remove unwanted impurities. Consequently, it avoids undergoing chemical transformations that could result in significant CO_2 release. Highlighting these differences, the advantages of utilizing SDE-based geopolymeric mortar over conventional cementitious alternatives become evident again, further underscoring its benefits.

6. CONCLUSIONS AND FUTURE RESEARCH

6.1. CONCLUSION

Based on the comprehensive analysis, it can be concluded that SDE is a viable silica source for geopolymer precursors, demonstrating that it is possible to produce geopolymers from SDE and apply them in mortar, being able to expand its use to other areas, such as wastewater treatment, as suggested by the literature. Remarkably, being a solid waste, its utilization significantly reduces the need for extracting natural resources.

Moreover, incorporating this geopolymer as a partial or complete binder in mortar formulations has produced promising materials with potential for future applications in civil construction. Further enhancements can be achieved by combining it with other aluminosilicates. This approach holds the promise of a more sustainable trajectory for the construction industry, promoting sustainable development and circular economy principles. The geopolymeric mortars developed display superior energy efficiency compared to traditional cementitious counterparts, as relevant literature shows. Additionally, it demonstrate a significantly reduced carbon dioxide emission footprint, contrasting with the substantial CO_2 emissions associated with cement production.

Chemical analysis revealed a higher degree of geopolymerization in GP2, which can contribute to improved mechanical properties, highlighting the immense potential of the material. In addition to these advantages, when comparing the different mortar samples produced, one sample, S2, stood out prominently due to its superior mechanical properties, achieving a value of 4,48 MPa of compressive strength. This particular sample comprises a binder with 75% of geopolymer GP2 and 25% of cement.

6.2. FUTURE RESEARCH

Concluding the possibility of producing geopolymers and geopolymeric mortars with SDE, it would be valuable for future research to explore the adherence and durability of these materials. Also, conducting a study about the incorporation of other aluminosilicates to enhance their mechanical properties, particularly in the case of binders composed solely of geopolymer, would be highly recommended. Furthermore, investigating these materials' heat and fire resistance is crucial, given their potential applications in civil construction, passive fire protection, and thermal insulation.

Moreover, the identified geopolymer GP2 with a significant specific surface area opens up possibilities for alternative applications beyond mechanical properties. For instance, its potential as an effective adsorbent in wastewater treatment could be further explored.

In conclusion, conducting a study on the actual environmental impact of reducing the accumulated SDE in landfills, especially now that it's proven that it can be repurposed for other applications even after being transformed into waste, would be highly beneficial.

7. REFERENCES

1. Benhelal, E., Shamsaei, E. & Rashid, M. I. Challenges against CO2 abatement strategies in cement industry: A review. *Journal of Environmental Sciences* **104**, 84–101 (2021).

2. Pendrill, F. *et al.* Agricultural and forestry trade drives large share of tropical deforestation emissions. *Global Environmental Change* **56**, 1–10 (2019).

3. Xu, B. & Lin, B. How industrialization and urbanization process impacts on CO 2 emissions in China: Evidence from nonparametric additive regression models. *Energy Econ* **48**, 188–202 (2015).

4. Yin, X. *et al.* China's transportation energy consumption and CO2 emissions from a global perspective. *Energy Policy* **82**, 233–248 (2015).

5. Al-Ghussain, L. Global warming: review on driving forces and mitigation. *Environ Prog Sustain Energy* **38**, 13–21 (2019).

6. United Nations Environment Programme. Global Status Report for Buildings and Construction: Towards a Zero-emission, Efficient and Resilient Buildings and Construction Sector. (2020).

7. Scrivener, K. L., John, V. M. & Gartner, E. M. Eco-efficient cements: Potential economically viable solutions for a low-CO2 cement-based materials industry. *Cem Concr Res* **114**, 2–26 (2018).

8. Singh, N. B. & Middendorf, B. Geopolymers as an alternative to Portland cement: An overview. *Constr Build Mater* **237**, 117455 (2020).

9. Krausmann, F., Lauk, C., Haas, W. & Wiedenhofer, D. From resource extraction to outflows of wastes and emissions: The socioeconomic metabolism of the global economy, 1900–2015. *Global Environmental Change* **52**, 131–140 (2018).

10. Bajželj, B., Allwood, J. M. & Cullen, J. M. Designing Climate Change Mitigation Plans That Add Up. *Environ Sci Technol* **47**, 8062–8069 (2013).

11. Habert, G. *et al.* Environmental impacts and decarbonization strategies in the cement and concrete industries. *Nat Rev Earth Environ* **1**, 559–573 (2020).

12. Friedlingstein, P. *et al.* Global Carbon Budget 2021. *Earth Syst Sci Data* **14**, 1917–2005 (2022).

13. Imbabi, M. S., Carrigan, C. & McKenna, S. Trends and developments in green cement and concrete technology. *International Journal of Sustainable Built Environment* **1**, 194–216 (2012).

14. Gomez-Zamorano, L. Y., Vega-Cordero, E. & Struble, L. Composite geopolymers of metakaolin and geothermal nanosilica waste. *Constr Build Mater* **115**, 269–276 (2016).

15. Tan, T. H., Mo, K. H., Ling, T.-C. & Lai, S. H. Current development of geopolymer as alternative adsorbent for heavy metal removal. *Environ Technol Innov* **18**, 100684 (2020).

16. Maddalena, R., Roberts, J. J. & Hamilton, A. Can Portland cement be replaced by low-carbon alternative materials? A study on the thermal properties and carbon emissions of innovative cements. *J Clean Prod* **186**, 933–942 (2018).

17. N Roussel. *Understanding the Rheology of Concrete*. (2011).

18. Arizzi, A. & Cultrone, G. Mortars and plasters—how to characterise hydraulic mortars. *Archaeol Anthropol Sci* **13**, 144 (2021).

19. EUROPEAN COMMITTEE FOR STANDARDIZATION. EN 196-1: Methods of testing cement. Preprint at (2006).

20. Davidovits, J. Geopolymers and geopolymeric materials. *Journal of Thermal Analysis* **35**, 429–441 (1989).

21. Duxson, P. *et al.* Geopolymer technology: the current state of the art. *J Mater Sci* **42**, 2917–2933 (2007).

22. Parthiban, D. *et al.* Role of industrial based precursors in the stabilization of weak soils with geopolymer – A review. *Case Studies in Construction Materials* **16**, e00886 (2022).

23. Hu, S. *et al.* Synthesis of rare earth tailing-based geopolymer for efficiently immobilizing heavy metals. *Constr Build Mater* **254**, 119273 (2020).

24. Ren, B. *et al.* Eco-friendly geopolymer prepared from solid wastes: A critical review. *Chemosphere* **267**, 128900 (2021).

25. Zhang, M., Deskins, N. A., Zhang, G., Cygan, R. T. & Tao, M. Modeling the Polymerization Process for Geopolymer Synthesis through Reactive Molecular Dynamics Simulations. *The Journal of Physical Chemistry C* **122**, 6760–6773 (2018).

26. J. Davidovits. Why Alkali-Activated Materials (AAM) are Not Geopolymers. *Geopolymer Institute Library* **Technical Paper #25**, (2018).

27. Komljenović, M., Baščarević, Z. & Bradić, V. Mechanical and microstructural properties of alkali-activated fly ash geopolymers. *J Hazard Mater* **181**, 35–42 (2010).

28. Wan, Q. *et al.* Geopolymerization reaction, microstructure and simulation of metakaolin-based geopolymers at extended Si/Al ratios. *Cem Concr Compos* **79**, 45–52 (2017).

29. Ahmari, S. & Zhang, L. Production of eco-friendly bricks from copper mine tailings through geopolymerization. *Constr Build Mater* **29**, 323–331 (2012).

30. Duxson, P., Mallicoat, S. W., Lukey, G. C., Kriven, W. M. & van Deventer, J. S. J. The effect of alkali and Si/Al ratio on the development of mechanical properties of metakaolin-based geopolymers. *Colloids Surf A Physicochem Eng Asp* **292**, 8–20 (2007).

31. Silva, P. de, Sagoe-Crenstil, K. & Sirivivatnanon, V. Kinetics of geopolymerization: Role of Al2O3 and SiO2. *Cem Concr Res* **37**, 512–518 (2007).

32. Rowles, M. & O'Connor, B. Chemical optimisation of the compressive strength of aluminosilicate geopolymers synthesised by sodium silicate activation of metakaolinite. *J Mater Chem* **13**, 1161–1165 (2003).

33. Ahmad Zaidi, F. H. *et al.* Geopolymer as underwater concreting material: A review. *Constr Build Mater* **291**, 123276 (2021).

34. Nurruddin, et al. Methods of curing geopolymer concrete: A review. *International Journal of ADVANCED AND APPLIED SCIENCES* **5**, 31–36 (2018).

35. Singh, B., Ishwarya, G., Gupta, M. & Bhattacharyya, S. K. Geopolymer concrete: A review of some recent developments. *Constr Build Mater* **85**, 78–90 (2015).

36. Nuruddin, M. F., Malkawi, A. B., Fauzi, A., Mohammed, B. S. & Al-Mattarneh, H. M. Effects of alkaline solution on the microstructure of HCFA geopolymers. in *Engineering Challenges for Sustainable Future* 501–505 (CRC Press, 2016). doi:10.9774/gleaf.9781315375052_96.

37. Singh, N. Fly Ash-Based Geopolymer Binder: A Future Construction Material. *Minerals* **8**, 299 (2018).

38. Wagners. Wagners EFC Home. https://www.wagner.com.au/main/what-we-do/earth-friendly-concrete/efc-home/ (2022).

39. Gao, H. *et al.* A bifunctional hierarchical porous kaolinite geopolymer with good performance in thermal and sound insulation. *Constr Build Mater* **251**, 118888 (2020).

40. Singh, S., Aswath, M. U. & Ranganath, R. V. Performance assessment of bricks and prisms: Red mud based geopolymer composite. *Journal of Building Engineering* **32**, 101462 (2020).

41. Rattanasak, U., Pankhet, K. & Chindaprasirt, P. Effect of chemical admixtures on properties of high-calcium fly ash geopolymer. *International Journal of Minerals, Metallurgy, and Materials* **18**, 364–369 (2011).

42. Liew, Y.-M., Heah, C.-Y., Mohd Mustafa, A. B. & Kamarudin, H. Structure and properties of clay-based geopolymer cements: A review. *Prog Mater Sci* **83**, 595–629 (2016).

43. Chindaprasirt, P., Jaturapitakkul, C., Chalee, W. & Rattanasak, U. Comparative study on the characteristics of fly ash and bottom ash geopolymers. *Waste Management* **29**, 539–543 (2009).

44. Cheng, T. W. & Chiu, J. P. Fire-resistant geopolymer produced by granulated blast furnace slag. *Miner Eng* **16**, 205–210 (2003).

45. Villa, C., Pecina, E. T., Torres, R. & Gómez, L. Geopolymer synthesis using alkaline activation of natural zeolite. *Constr Build Mater* **24**, 2084–2090 (2010).

46. Pimraksa, K., Chindaprasirt, P., Rungchet, A., Sagoe-Crentsil, K. & Sato, T. Lightweight geopolymer made of highly porous siliceous materials with various Na2O/Al2O3 and SiO2/Al2O3 ratios. *Materials Science and Engineering: A* **528**, 6616–6623 (2011).

47. Song, Q., Li, J. & Zeng, X. Minimizing the increasing solid waste through zero waste strategy. *J Clean Prod* **104**, 199–210 (2015).

48. Guerrero, L. A., Maas, G. & Hogland, W. Solid waste management challenges for cities in developing countries. *Waste Management* **33**, 220–232 (2013).

49. MEE. National Annual Report of Solid Waste Pollution Prevention and Control in Big and Medium-Sized Cities (in chinese). Preprint at (2019).

50. Morseletto, P. Targets for a circular economy. *Resour Conserv Recycl* **153**, 104553 (2020).

51. Rosenboom, J.-G., Langer, R. & Traverso, G. Bioplastics for a circular economy. *Nat Rev Mater* **7**, 117–137 (2022).

52. Nandi, S., Sarkis, J., Hervani, A. A. & Helms, M. M. Redesigning Supply Chains using Blockchain-Enabled Circular Economy and COVID-19 Experiences. *Sustain Prod Consum* **27**, 10–22 (2021).

53. Wang, T., Ishida, T. & Gu, R. A study of the influence of crystal component on the reactivity of low-calcium fly ash in alkaline conditions based on SEM-EDS. *Constr Build Mater* **243**, 118227 (2020).

54. Gupta, V., Pathak, D. K., Siddique, S., Kumar, R. & Chaudhary, S. Study on the mineral phase characteristics of various Indian biomass and coal fly ash for its use in masonry construction products. *Constr Build Mater* **235**, 117413 (2020).

55. Duan, P., Yan, C. & Zhou, W. Compressive strength and microstructure of fly ash based geopolymer blended with silica fume under thermal cycle. *Cem Concr Compos* **78**, 108–119 (2017).

56. Geng, J. *et al.* Comparison of red mud and coal gangue blended geopolymers synthesized through thermal activation and mechanical grinding preactivation. *Constr Build Mater* **153**, 185–192 (2017).

57. Abdel-Ghani, N. T., Elsayed, H. A. & AbdelMoied, S. Geopolymer synthesis by the alkali-activation of blastfurnace steel slag and its fire-resistance. *HBRC Journal* **14**, 159–164 (2018).

58. Wei, B., Zhang, Y. & Bao, S. Preparation of geopolymers from vanadium tailings by mechanical activation. *Constr Build Mater* **145**, 236–242 (2017).

59. Duan, P., Yan, C., Zhou, W. & Ren, D. Fresh properties, compressive strength and microstructure of fly ash geopolymer paste blended with iron ore tailing under thermal cycle. *Constr Build Mater* **118**, 76–88 (2016).

60. Song, M., Jiaping, L., Qian, J., Jianzhong, L. & Liang, S. Experimental Study on Utilization of Quartz Mill Tailings as a Filler to Prepare Geopolymer. *Mineral Processing and Extractive Metallurgy Review* **37**, 311–322 (2016).

61. Liang, G., Zhu, H., Zhang, Z., Wu, Q. & Du, J. Investigation of the waterproof property of alkali-activated metakaolin geopolymer added with rice husk ash. *J Clean Prod* **230**, 603–612 (2019).

62. Salih, M. A., Abang Ali, A. A. & Farzadnia, N. Characterization of mechanical and microstructural properties of palm oil fuel ash geopolymer cement paste. *Constr Build Mater* **65**, 592–603 (2014).

63. Novais, R. M. *et al.* High pH buffer capacity biomass fly ash-based geopolymer spheres to boost methane yield in anaerobic digestion. *J Clean Prod* **178**, 258–267 (2018).

64. Zhu, W., Rao, X. H., Liu, Y. & Yang, E.-H. Lightweight aerated metakaolin-based geopolymer incorporating municipal solid waste incineration bottom ash as gas-forming agent. *J Clean Prod* **177**, 775–781 (2018).

65. Toniolo, N. *et al.* Extensive reuse of soda-lime waste glass in fly ash-based geopolymers. *Constr Build Mater* **188**, 1077–1084 (2018).

66. Korunic, Z. Review Diatomaceous earths, a group of natural insecticides. *J Stored Prod Res* **34**, 87–97 (1998).

67. Zeni, V., Baliota, G. V., Benelli, G., Canale, A. & Athanassiou, C. G. Diatomaceous Earth for Arthropod Pest Control: Back to the Future. *Molecules* **26**, 7487 (2021).

68. Korunic, Z. Overview of undesirable effects of using diatomaceous earths for direct mixing with grains. *Pesticidi i fitomedicina* **31**, 9–18 (2016).

69. Reka, A. A. *et al.* Diatomaceous Earth: Characterization, thermal modification, and application. *Open Chem* **19**, 451–461 (2021).

70. Terra de diatomáceas: características, tipos e aplicações. https://lojahusqvarna.com (2022).

71. Shah, M. A. & Khan, A. A. Use of diatomaceous earth for the management of stored-product pests. *Int J Pest Manag* **60**, 100–113 (2014).

72. Ribéreau-Gayon, P., Glories, Y., Maujean, A. & Dubourdieu, D. Clarifying Wine by Filtration and Centrifugation. in *Handbook of Enology* 333–367 (John Wiley & Sons, Ltd, 2006). doi:10.1002/0470010398.ch11.

73. Arbi, K., Palomo, A. & Fernández-Jiménez, A. Alkali-activated blends of calcium aluminate cement and slag/diatomite. *Ceram Int* **39**, 9237–9245 (2013).

74. Pimraksa, K., Chindaprasirt, P., Rungchet, A., Sagoe-Crentsil, K. & Sato, T. Lightweight geopolymer made of highly porous siliceous materials with various Na2O/Al2O3 and SiO2/Al2O3 ratios. *Materials Science and Engineering: A* **528**, 6616–6623 (2011).

75. Mejía, J. M., Mejía de Gutiérrez, R. & Montes, C. Rice husk ash and spent diatomaceous earth as a source of silica to fabricate a geopolymeric binary binder. *J Clean Prod* **118**, 133–139 (2016).

76. Font, A. *et al.* Use of residual diatomaceous earth as a silica source in geopolymer production. *Mater Lett* **223**, 10–13 (2018).

77. Albitar, M., Mohamed Ali, M. S., Visintin, P. & Drechsler, M. Durability evaluation of geopolymer and conventional concretes. *Constr Build Mater* **136**, 374–385 (2017).

78. Castel, A. & Foster, S. J. Bond strength between blended slag and Class F fly ash geopolymer concrete with steel reinforcement. *Cem Concr Res* **72**, 48–53 (2015).

79. Zhang, P., Wang, K., Wang, J., Guo, J. & Ling, Y. Macroscopic and microscopic analyses on mechanical performance of metakaolin/fly ash based geopolymer mortar. *J Clean Prod* **294**, 126193 (2021).

80. Huseien, G. F., Mirza, J., Ismail, M., Ghoshal, S. K. & Ariffin, M. A. M. Effect of metakaolin replaced granulated blast furnace slag on fresh and early strength properties of geopolymer mortar. *Ain Shams Engineering Journal* **9**, 1557–1566 (2018).

81. Phoo-ngernkham, T., Maegawa, A., Mishima, N., Hatanaka, S. & Chindaprasirt, P. Effects of sodium hydroxide and sodium silicate solutions on compressive and shear bond strengths of FA–GBFS geopolymer. *Constr Build Mater* **91**, 1–8 (2015).

82. Hawa, A., Tonnayopas, D. & Prachasaree, W. Performance Evaluation and Microstructure Characterization of Metakaolin-Based Geopolymer Containing Oil Palm Ash. *The Scientific World Journal* **2013**, 1–9 (2013).

83. Karim, Md. *et al.* On the Utilization of Pozzolanic Wastes as an Alternative Resource of Cement. *Materials* **7**, 7809–7827 (2014).

84. Miranda, J. M., Fernández-Jiménez, A., González, J. A. & Palomo, A. Corrosion resistance in activated fly ash mortars. *Cem Concr Res* **35**, 1210–1217 (2005).

85. El-Sayed, H. A., El-Enein, S. A. A., Khate, H. M. & Hasanein, S. A. Resistance of alkali activated water-cooled slaggeopolymer to sulphate attack. *Ceramics - Silikaty* 153–160 (2011).

86. Prabu, B., Shalini, A. & Kumar, J. K. Rice husk ash based geopolymer concrete-a review. *Chem. Sci. Rev. Lett.* **3**, 288–294 (2014).

87. Revathy, V. & Antherjanam, G. Strength Comparison of Cement Mortar and Geopolymer Mortar. in 175–182 (2020). doi:10.1007/978-3-030-26365-2_17.

88. Zhang, H. Y., Qiu, G. H., Kodur, V. & Yuan, Z. S. Spalling behavior of metakaolin-fly ash based geopolymer concrete under elevated temperature exposure. *Cem Concr Compos* **106**, 103483 (2020).

89. Zhang, P. *et al.* Mechanical properties and prediction of fracture parameters of geopolymer/alkali-activated mortar modified with PVA fiber and nano-SiO2. *Ceram Int* **46**, 20027–20037 (2020).

90. Pacheco-Torgal, F., Moura, D., Ding, Y. & Jalali, S. Composition, strength and workability of alkali-activated metakaolin based mortars. *Constr Build Mater* **25**, 3732–3745 (2011).

91. Villca, A. R. *et al.* Hybrid Lime–Pozzolan Geopolymer Systems: Microstructural, Mechanical and Durability Studies. *Materials* **15**, 2736 (2022).

92. Bouzón, N. *et al.* Refluxed rice husk ash/NaOH suspension for preparing alkali activated binders. *Mater Lett* **115**, 72–74 (2014).

93. Méndez, R., Borrachero, M. V., Payá, J. & Monzó, J. M. Mechanical Strength of Lime-Rice Husk Ash Mortars: A Preliminary Study. *Key Eng Mater* **517**, 495–499 (2012).

94. Habert, G., d'Espinose de Lacaillerie, J. B. & Roussel, N. An environmental evaluation of geopolymer based concrete production: reviewing current research trends. *J Clean Prod* **19**, 1229–1238 (2011).

95. Novaes, C. G. *et al.* A review of multivariate designs applied to the optimization of methods based on inductively coupled plasma optical emission spectrometry (ICP OES). *Microchemical Journal* **128**, 331–346 (2016).

96. Riaz, T. *et al.* FTIR analysis of natural and synthetic collagen. *Appl Spectrosc Rev* **53**, 703–746 (2018).

97. Ermrich, Martin. & Opper, Detlef. *XRD for the analyst : getting acquainted with the principles*. (2011).

98. Goldstein, J. *Practical Scanning Electron Microscopy*. *Practical Scanning Electron Microscopy* (Springer US, 1975). doi:10.1007/978-1-4613-4422-3.

99. Thommes, M. *et al.* Physisorption of gases, with special reference to the evaluation of surface area and pore size distribution (IUPAC Technical Report). *Pure and Applied Chemistry* **87**, 1051–1069 (2015).

100. EUROPEAN COMMITTEE FOR STANDARDIZATION. EN 1015-11: Methods of test for mortar for masonry - Part 11: Determination of flexural and compressive strength of hardened mortar. Preprint at (2019).

101. EUROPEAN COMMITTEE FOR STANDARDIZATION. EN 1015-3: Methods of test for mortar for masonry — Part 3: Determination of consistence of fresh mortar (by flow table). Preprint at (2004).

102. American Society for Testing and Materials. ASTM C 1437: Test Method for Flow of Hydraulic Cement Mortar. (2020).

103. Vennapusa, J. R., Konala, A., Dixit, P. & Chattopadhyay, S. Caprylic acid based PCM composite with potential for thermal buffering and packaging applications. *Mater Chem Phys* **253**, 123453 (2020).

104. Baturin, G. N. Comparison of elemental composition of recent and ancient carbonaceous sediments. *Doklady Earth Sciences* **444**, 729–733 (2012).

105. Nath, S. K. & Kumar, S. Role of particle fineness on engineering properties and microstructure of fly ash derived geopolymer. *Constr Build Mater* **233**, 117294 (2020).

106. Xiao, R. *et al.* Strength, microstructure, efflorescence behavior and environmental impacts of waste glass geopolymers cured at ambient temperature. *J Clean Prod* **252**, 119610 (2020).

107. Tsai, W.-T., Lai, C.-W. & Hsien, K.-J. Characterization and adsorption properties of diatomaceous earth modified by hydrofluoric acid etching. *J Colloid Interface Sci* **297**, 749–754 (2006).

108. Li, S., Li, D., Su, F., Ren, Y. & Qin, G. Uniform surface modification of diatomaceous earth with amorphous manganese oxide and its adsorption characteristics for lead ions. *Appl Surf Sci* **317**, 724–729 (2014).

109. Falaras, P., Kovanis, I., Lezou, F. & Seiragakis, G. Cottonseed oil bleaching by acid-activated montmorillonite. *Clay Miner* **34**, 221–232 (1999).

110. Vassileva, P. *et al. CHARACTERIZATION OF NATURAL DIATOMITES FROM BULGARIA*. (2011).

111. Churata, R. *et al.* Study of Geopolymer Composites Based on Volcanic Ash, Fly Ash, Pozzolan, Metakaolin and Mining Tailing. *Buildings* **12**, 1118 (2022).

112. Inchaurrondo, N., Font, J., Ramos, C. P. & Haure, P. Natural diatomites: Efficient green catalyst for Fenton-like oxidation of Orange II. *Appl Catal B* **181**, 481–494 (2016).

113. KHRAISHEH, M., ALDEGS, Y. & MCMINN, W. Remediation of wastewater containing heavy metals using raw and modified diatomite. *Chemical Engineering Journal* **99**, 177–184 (2004).

114. Touina, A. *et al.* Characterization and efficient dye discoloration of Algerian diatomite from Ouled Djilali-Mostaganem. *SN Appl Sci* **3**, 476 (2021).

115. Matovic, B., Saponjic, A., Devecerski, A. & Miljkovic, M. Fabrication of SiC by carbothermal-reduction reactions of diatomaceous earth. *J Mater Sci* **42**, 5448–5451 (2007).

116. Diaz, E. I., Allouche, E. N. & Eklund, S. Factors affecting the suitability of fly ash as source material for geopolymers. *Fuel* **89**, 992–996 (2010).

117. Kirschner, A. V & Harmuth, H. *INVESTIGATION OF GEOPOLYMER BINDERS WITH RESPECT TO THEIR APPLICATION FOR BUILDING MATERIALS*. *Original papers Ceramics − Silikáty* vol. 48 (2004).

118. Gregg S. J, K. S. W. S. Adsorption, surface area, and porosity. *Academic Press* (1982).

119. He, P. *et al.* Effects of Si/Al ratio on the structure and properties of metakaolin based geopolymer. *Ceram Int* **42**, 14416–14422 (2016).

120. Han, W. *et al.* Effects of Al/Na and Si/Na Molar Ratios on the Alkalinity of Metakaolin-Based Geopolymer Pore Solutions. *Materials* **16**, 1929 (2023).

121. Ibrahim, W. M. W., Hussin, K., Abdullah, M. M. A., Kadir, A. A. & Deraman, L. M. Effects of sodium hydroxide (NaOH) solution concentration on fly ash-based lightweight geopolymer. in 020011 (2017). doi:10.1063/1.5002205.

122. Yahya, Z., Abdullah, M. M. A. B., Talib, S. Z. A. & Razak, R. A. Comparative study on early strength of sodium hydroxide (NaOH) activated fly ash based geopolymer. in 020059 (2017). doi:10.1063/1.5003542.

123. Swanson & Howard E. *Standard X-ray Diffraction Powder Patterns UNITED STATES DEPARTMENT OF COMMERCE NATIONAL BUREAU OF STANDARDS*. (1960).

124. Feret, F. R., Roy, D. & Boulanger, C. Determination of alpha and beta alumina in ceramic alumina by X-ray diffraction. *Spectrochim Acta Part B At Spectrosc* **55**, 1051–1061 (2000).

125. Tchakoute Kouamo, H., Elimbi, A., Mbey, J. A., Ngally Sabouang, C. J. & Njopwouo, D. The effect of adding alumina-oxide to metakaolin and volcanic ash on geopolymer products: A comparative study. *Constr Build Mater* **35**, 960–969 (2012).

126. Tchakoute Kouamo, H., Elimbi, A., Mbey, J. A., Ngally Sabouang, C. J. & Njopwouo, D. The effect of adding alumina-oxide to metakaolin and volcanic ash on geopolymer products: A comparative study. *Constr Build Mater* **35**, 960–969 (2012).

127. Yang, J., Li, D. & Fang, Y. Synthesis of Nanoscale CaO-Al2O3-SiO2-H2O and Na2O-Al2O3-SiO2-H2O Using the Hydrothermal Method and Their Characterization. *Materials* **10**, 695 (2017).

128. Ryu, G. S., Lee, Y. B., Koh, K. T. & Chung, Y. S. The mechanical properties of fly ash-based geopolymer concrete with alkaline activators. *Constr Build Mater* **47**, 409–418 (2013).

129. Tanhaei, B., Ayati, A., Lahtinen, M. & Sillanpää, M. Preparation and characterization of a novel chitosan/Al2O3/magnetite nanoparticles composite adsorbent for kinetic, thermodynamic and isotherm studies of Methyl Orange adsorption. *Chemical Engineering Journal* **259**, 1–10 (2015).

130. Çelikten, S. & Işıkdağ, B. Strength Development of Ground Perlite-Based Geopolymer Mortars. *Advances in Concrete Construction* **9**, 227–234 (2020).

131. Zheng, Z., Ma, X., Zhang, Z. & Li, Y. In-situ transition of amorphous gels to Na-P1 zeolite in geopolymer: Mechanical and adsorption properties. *Constr Build Mater* **202**, 851–860 (2019).

132. Garcia-Lodeiro, I., Palomo, A., Fernández-Jiménez, A. & Macphee, D. E. Compatibility studies between N-A-S-H and C-A-S-H gels. Study in the ternary diagram Na2O–CaO–Al2O3–SiO2–H2O. *Cem Concr Res* **41**, 923–931 (2011).

133. De Silva, P. & Sagoe-Crenstil, K. Medium-term phase stability of Na2O–Al2O3–SiO2–H2O geopolymer systems. *Cem Concr Res* **38**, 870–876 (2008).

134. Sathonsaowaphak, A., Chindaprasirt, P. & Pimraksa, K. Workability and strength of lignite bottom ash geopolymer mortar. *J Hazard Mater* **168**, 44–50 (2009).

135. Islam, A., Alengaram, U. J., Jumaat, M. Z. & Bashar, I. I. The development of compressive strength of ground granulated blast furnace slag-palm oil fuel ash-fly ash based geopolymer mortar. *Materials & Design (1980-2015)* **56**, 833–841 (2014).

136. Guo, X., Shi, H. & Dick, W. A. Compressive strength and microstructural characteristics of class C fly ash geopolymer. *Cem Concr Compos* **32**, 142–147 (2010).

137. Ahmed, H. U. *et al.* Compressive Strength of Sustainable Geopolymer Concrete Composites: A State-of-the-Art Review. *Sustainability* **13**, 13502 (2021).

8. APPENDIX

8.1. APPENDIX I

8.1.1. Mechanical Strength

Table 14: Compressive Strength Values of Geopolymeric Mortars.

Samples	**Compressive Strength (MPa)**	**Error**
S1	4.05	0.18
S2	4.68	0.73
S3	3.41	0.23
S4	3.57	0.15
S5	0.92	0.04
S6	1.02	0.22
S7	1.25	0.22
S8	0.70	0.06
S9	1.97	0.67
S10	2.55	0.67
S11	1.72	0.62
S12	2.46	0.45

Table 15: Flexural Strength Values of Geopolymeric Mortars.

Samples	**Flexural Strength (MPa)**	**Error**
S1	1.04	0.47
S2	1.51	0.55
S3	1.12	0.33
S4	1.32	0.48
S5	0.22	0.02
S6	0.28	0.07
S7	0.28	0.05
S8	0.14	0.03
S9	0.23	0.07
S10	0.25	0.11
S11	0.11	0.03
S12	0.24	0.04

8.1.2. Workability

Table 16: Flow Test Values of Geopolymeric Mortars.

Samples	**Flow (%)**
S1	67
S2	63
S3	66
S4	65
S5	88
S6	87
S7	90
S8	82
S9	93
S10	87
S11	91
S12	90

8.2. APPENDIX II

Scientific Events Presentations

This work generated an oral presentation in two scientific events. The first one was the international congress XXVI Galician-Portuguese Chemistry Meeting – this congress has the aim of promoting scientific and technological exchange among university members, undergraduate/graduate students, doctoral students and postgraduate, researchers and chemical in the companies, contributing to the greater dissemination of technical and scientific knowledge.

The second event was the VII Young Researchers Meeting that took place at the Polytechnic Institute of Bragança (IPB). The aim is to promote the participation of students involved in research at IPB in events of a scientific nature, publicly presenting their research work and welcoming critical appreciation from the community.

The presentations abstracts are shown below.

Production and Characterization of Geopolymeric Mortars From Diatomaceous Earth

Júlia F. Murta[1,2,3*], Ana Paula Ferreira da Silva[1,2*], Leandro Magalhães[1], Debora Macanjo[1,4], Carlos Eduardo dos Santos.[3], Helder T. Gomes [1,2]

[1]Centro de Investigação de Montanha (CIMO), Instituto Politécnico de Bragança, Campus de Santa Apolónia, 5300-253 Bragança, Portugal

[2]Laboratório Associado para a Sustentabilidade e Tecnologia em Regiões de Montanha (SusTEC), Instituto Politécnico de Bragança, Campus de Santa Apolónia, 5300-253 Bragança, Portugal

[3] Departamento de Engenharia de Materiais, Centro Federal de Educação Tecnológica de Minas Gerais, 30421-169 Belo Horizonte, Brasil

[4] C-MADE Centro de Materiais e Tecnologia Construtivas, Universidade Beira Interior (UBI).

**anapaula.silva@ipb.pt*

Due to the high release of carbon dioxide into the atmosphere, the earth's average surface temperature has increased. Heat waves, melting of glaciers and animal deaths are some visible consequences. Deforestation, agriculture, transportation and industries are major contributors to CO_2 emissions [2]. For instance, Portland Cement generates high pollution levels, responsible for around 7% of global carbon dioxide emissions [3]. For this reason, Portland cement alternatives are needed to reduce these emissions. This study proposes the application of spent diatomaceous earth, a solid waste commonly used in the wine industry as a wine filtration agent, to produce geopolymer mortars.

Geopolymers are inorganic polymers produced from an aluminosilicate precursor and activated by an alkaline solution [4]. They have been studied as alternatives to cement in mortars and concretes. In this work, the geopolymer mortars were produced using spent diatomaceous earth and alumina as precursors, with a Si:Al ratio of 2:1. The activating solution was prepared with sodium hydroxide (NaOH) solution varying the concentration in 10 and 12 M, and sodium silicate in a mass ratio of 1:2, by mixing both with a magnetic stirrer for 10 minutes. Then, this activating solution was mixed with the precursors and distilled water in a standardized paddle mixer. After that, this geopolymer fluid was mixed with sand in a proportion of 1:3:0,85 (geopolymer:sand:water) in the same equipment.

After all the previous steps, the mortar was poured into molds of 40×40×160 mm. The curing process consisted of letting the samples in an oven at 40 ºC for 7 days, demolding them on the fourth day. Subsequently, compressive and bending tests were conducted, and the results are shown in Table 1. Sample G_10M was prepared with a NaOH solution of 10M, and sample G_12M with a solution of 12M.

The results show that using a higher concentration of sodium hydroxide increases compressive and flexural strength. It confirms the literature, as increasing the pH with higher concentrations of NaOH increases the dissolution and solubility of aluminosilicate precursors and provides positive ions to counterbalance the negative charge of the aluminate group [5]. Furthermore, according to the European Standard EN 998-1, with these strengths, both mortars can be defined as class III mortars [6].

Table 1. Mechanical properties of geopolymeric mortars

Sample	Compressive strength after 7 days (MPa)	Flexural strength after 7 days (MPa)
G_10M	4,35	3,11
G_12M	4,46	4,00

Acknowledgments

The authors are grateful to the Foundation for Science and Technology (FCT, Portugal) for financial support through national funds FCT/MCTES (PIDDAC) to CIMO (UIDB/00690/2020 and UIDP/00690/2020) and SusTEC (LA/P/0007/2020). This work is also a result of the project "BacchusTech - Integrated Approach for the Valorisation of Winemaking Residues" (POCI-01-0247-FEDER-069583), supported by the Competitiveness and Internationalization Operational Programme (COMPETE 2020), under the PORTUGAL 2020 Partnership Agreement, through the European Regional Development Fund (ERDF).

References

[1] Pendrill, F. et al.. Global Environmental Change 56 (2019) 1–10.

[2] Andrew, R. et al.. Earth Syst. Sci. Data 14 (2022) 1917–2005.

[3] Davidovits, J.. Journal of Thermal Analysis 35 (1989) 429–441.

[4] Pacheco-Torgal, F. et al.. Constr. Build. Mater. 25 (2011) 3732–3745.

[5] European Committee for Standardization. EN 998-1: Specification for mortar for masonry (2003).

Produção e caracterização de argamassas geopoliméricas com terra diatomácea residual

Júlia Ferreira Murta[1,2,3]; Ana Paula Ferreira da S.[1,2]; Carlos Eduardo dos Santos[3]; Débora R. de S. M. Ferreira[1,4]; Helder T Gomes[1,2*]

[1]Centro de Investigação de Montanha (CIMO), Instituto Politécnico de Bragança, Portugal; [2]Laboratório Associado para a Sustentabilidade e Tecnologia em Regiões de Montanha (SusTEC), Instituto Politécnico de Bragança, Portugal; [3]Departamento de Engenharia de Materiais, Centro Federal de Educação Tecnológica de Minas Gerais, Brasil; [4]C-MADE Centre of Materials and Building Technologie, The University of Beira Interior (UBI).

*htgomes@ipb.pt

Resumo

Devido à alta liberação de dióxido de carbono na atmosfera, a temperatura média da superfície da Terra aumentou. Entre os principais responsáveis por isso está a indústria de Cimento Portland, que gera altos níveis de poluição, emitindo cerca de 7% das emissões globais de CO_2. Por isso, alternativas ao cimento Portland são necessárias para reduzir essas emissões. Este estudo propõe a aplicação de terra diatomáceas, resíduo sólido comumente utilizado na indústria vinícola como agente de filtração de vinhos, para a produção de argamassas geopoliméricas (AGP). Neste trabalho, as AGPs foram produzidos usando terra diatomáceas residual e alumina como precursores, com razão Si:Al de 2:1. A solução ativante foi preparada com solução de NaOH variando a concentração em 10 e 12 M, e silicato de sódio na razão mássica de 1:2, misturou-se ambas soluções com agitador magnético por 10 minutos. Em seguida, esta solução ativante foi misturada com os precursores e água destilada em um misturador de pás padronizado. Em seguida, na proporção de 1:3:0,67 (binder:areia:água), misturou-se uma porcentagem de cimento (25% ou 10%) com o binder geopolimérico produzindo as AGPs. O processo de cura consistiu em deixar as amostras em moldes de 40×40×160 mm em estufa a 40 ºC por 4 dias, desmoldando-as no quarto dia e deixando-as em temperatura ambiente. Posteriormente, foram realizados ensaios de compressão e flexão após 28 dias de produção. Os resultados esperados são uma resistência mecânica da argamassa geopolimérica próxima à de uma argamassa cimentícia (5 a 25 MPa) e uma boa trabalhabilidade.

Palavras-chave: argamassas geopoliméricas; terra diatomácea; resíduo sólido.

Financiamento: Este trabalho foi suportado pela Fundação Portuguesa para a Ciência e Tecnologia (FCT, Portugal) para apoio financeiro através dos fundos nacionais FCT/MCTES (PIDDAC) ao CIMO (UIDB/00690/2020 e UIDP/00690/2020) e SusTEC (LA/P/0007 /2020). Este trabalho é também resultado do projeto "BacchusTech - Abordagem Integrada para a Valorização de Resíduos Vinícolas" (POCI-01-0247-FEDER-069583), apoiado pelo Programa Operacional Competitividade e Internacionalização (COMPETE 2020) , no âmbito do Acordo de Parceria PORTUGAL 2020, através do Fundo Europeu de Desenvolvimento Regional (FEDER).

Production and characterization of spent diatomaceous earth geopolymeric mortars

Júlia Ferreira Murta[1,2,3]; Ana Paula Ferreira da S.[1,2]; Carlos Eduardo dos Santos[3]; Débora R. de S. M. Ferreira[1,4]; Helder T Gomes[1,2*]

[1]Centro de Investigação de Montanha (CIMO), Instituto Politécnico de Bragança, Portugal; [2]Laboratório Associado para a Sustentabilidade e Tecnologia em Regiões de Montanha (SusTEC), Instituto Politécnico de Bragança, Portugal; [3]Departamento de Engenharia de Materiais, Centro Federal de Educação Tecnológica de Minas Gerais, Brasil; [4]C-MADE Centre of Materials and Building Technologie, The University of Beira Interior (UBI).

*htgomes@ipb.pt

Abstract

Due to the high release of carbon dioxide into the atmosphere, the earth's average surface temperature has increased. Among the main responsible for this is the Portland Cement industry, which generates high pollution levels, emitting around 7% of global CO_2 emissions. For this reason, Portland cement alternatives are needed to reduce these emissions. This study proposes the application of spent diatomaceous earth, a solid waste commonly used in the winery industry as a wine filtration agent, to produce geopolymeric mortars (GPM). In this work, the GPMs were produced using spent diatomaceous earth and alumina as precursors, with a Si:Al ratio of 2:1. The activating solution was prepared with NaOH solution varying the concentration in 10 and 12 M, and sodium silicate in a mass ratio of 1:2, mixing both in with a magnetic stirrer for 10 minutes. Then, this activating solution was mixed with the precursors and distilled water in a standardized paddle mixer. After that, in a proportion of 1:3:0,67 (binder:sand:water), a percentage of cement (25% or 10%) was mixed with the geopolymer binder producing the geopolymeric mortars. The curing process consisted of letting the samples into molds of 40×40×160 mm in an oven at 40 ºC for 4 days, demoulding them on the fourth day and letting them at room temperature. Subsequently, compressive and bending tests were conducted after 28 days of production. The expected results are a mechanical strength of the geopolymer mortar close to that of a cementitious mortar (5 to 25MPa) and a good workability.

Keywords: geopolymeric mortars; diatomaceous earth; solid waste.

Funding: This work was supported by the Portuguese Foundation for Science and Technology (FCT) for financial support through national funds FCT/MCTES (PIDDAC) to CIMO (UIDB/00690/2020 and UIDP/00690/2020) and SusTEC (LA/P/0007/2020). This work is also a result of the project "BacchusTech - Integrated Approach for the Valorisation of Winemaking Residues" (POCI-01-0247-FEDER-069583), supported by the Competitiveness and Internationalization Operational Programme (COMPETE 2020), under the PORTUGAL 2020 Partnership Agreement, through the European Regional Development Fund (ERDF).